Ground-Water Chemistry and Diagenetic Reactions in Tertiary Sandstones of the Green River and Wasatch Formations, Uinta Basin, Utah

U.S. GEOLOGICAL SURVEY BULLETIN 1787-X

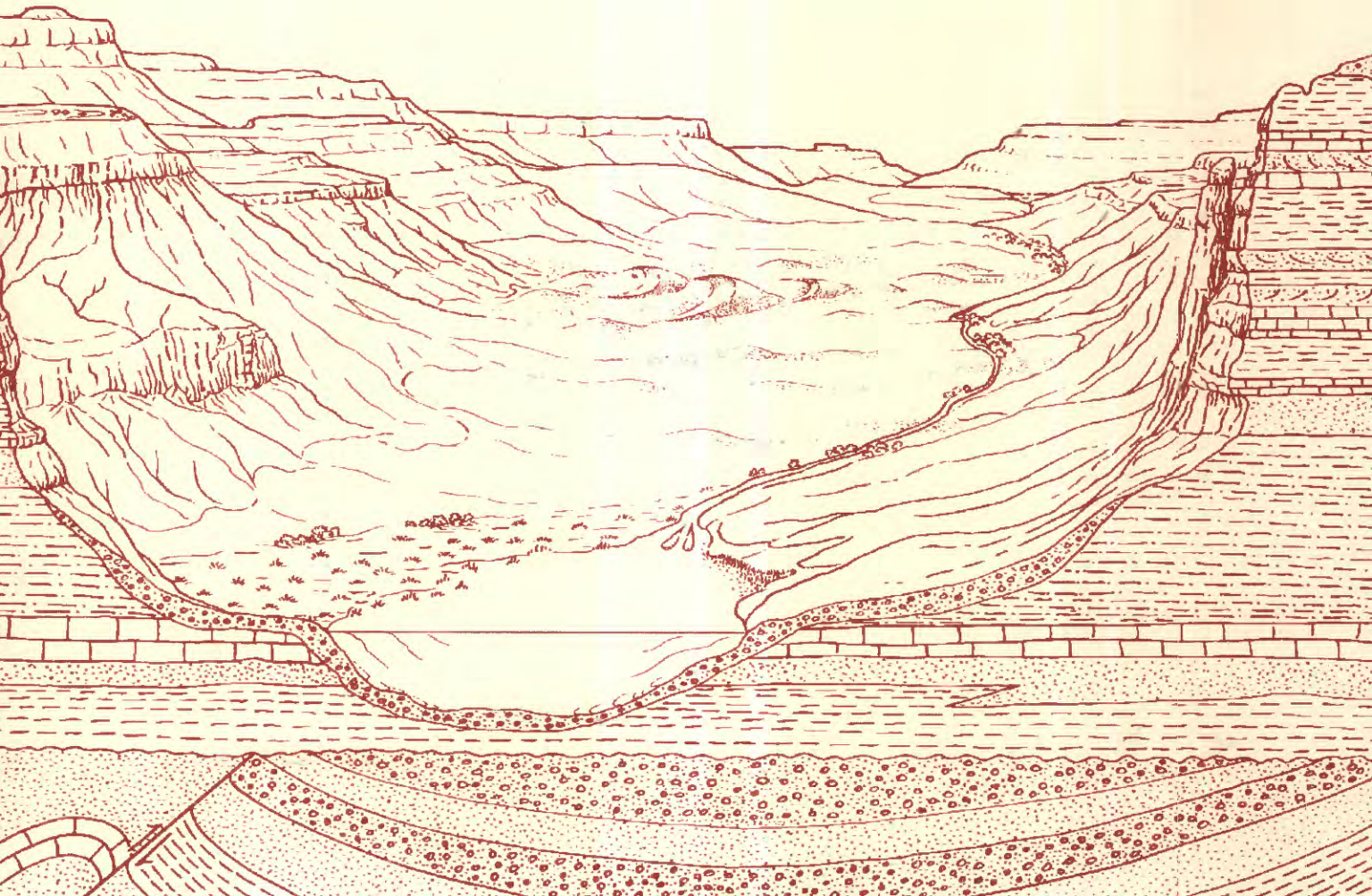

AVAILABILITY OF BOOKS AND MAPS OF THE U.S. GEOLOGICAL SURVEY

Instructions on ordering publications of the U.S. Geological Survey, along with the last offerings, are given in the current-year issues of the monthly catalog "New Publications of the U.S. Geological Survey." Prices of available U.S. Geological Survey publications released prior to the current year are listed in the most recent annual "Price and Availability List." Publications that are listed in various U.S. Geological Survey catalogs (**see back inside cover**) but not listed in the most recent annual "Price and Availability List" are no longer available.

Prices of reports released to the open files are given in the listing "U.S. Geological Survey Open-File Reports," updated monthly, which is for sale in microfiche from the U.S. Geological Survey, Books and Open-File Reports Section, Federal Center, Box 25425, Denver, CO 80225. Reports released through the NTIS may be obtained by writing to the National Technical Information Service, U.S. Department of Commerce, Springfield, VA 22161; please include NTIS report number with inquiry.

Order U.S. Geological Survey publications **by mail** or **over the counter** from the offices given below.

BY MAIL

Books

Professional Papers, Bulletins, Water-Supply Papers, Techniques of Water-Resources Investigations, Circulars, publications of general interest (such as leaflets, pamphlets, booklets), single copies of periodicals (Earthquakes & Volcanoes, Preliminary Determination of Epicenters), and some miscellaneous reports, including some of the foregoing series that have gone out of print at the Superintendent of Documents, are obtainable by mail from

U.S. Geological Survey, Books and Open-File Reports Section
Federal Center, Box 25425
Denver, CO 80225

Subscriptions to periodicals (Earthquakes & Volcanoes and Preliminary Determination of Epicenters) can be obtained ONLY from

Superintendent of Documents
U.S. Government Printing Office
Washington, DC 20402

(Check or money order must be payable to Superintendent of Documents.)

Maps

For maps, address mail orders to

U.S. Geological Survey, Map Distribution
Federal Center, Box 25286
Denver, CO 80225

Residents of Alaska may order maps from

U.S. Geological Survey, Map Distribution
New Federal Building - Box 12
101 Twelfth Ave., Fairbanks, AK 99701

OVER THE COUNTER

Books

Books of the U.S. Geological Survey are available over the counter at the following U.S. Geological Survey offices, all of which are authorized agents of the Superintendent of Documents:

- **ANCHORAGE, Alaska**—4230 University Dr., Rm. 101
- **ANCHORAGE, Alaska**—605 West 4th Ave., Rm. G–84
- **DENVER, Colorado**—Federal Bldg., Rm. 169, 1961 Stout St.
- **LOS ANGELES, California**—Federal Bldg., Rm. 7638, 300 North Los Angeles St.
- **MENLO PARK, California**—Bldg. 3, Rm. 3128, 345 Middlefield Rd.
- **RESTON, Virginia**—National Center, Rm. 1C402, 12201 Sunrise Valley Dr.
- **SALT LAKE CITY, Utah**—Federal Bldg., Rm. 8105, 125 South State St.
- **SAN FRANCISCO, California**—Customhouse, Rm. 504, 555 Battery St.
- **SPOKANE, Washington**—U.S. Courthouse, Rm. 678, West 920 Riverside Ave.
- **WASHINGTON, DC**—U.S. Department of the Interior Bldg., Rm. 2650, 1849 C St., NW.

Maps

Maps may be purchased over the counter at the U.S. Geological Survey offices where books are sold (all addresses in above list) and at the following U.S. Geological Survey offices:

- **ROLLA, Missouri**—1400 Independence Rd.
- **FAIRBANKS, Alaska**—New Federal Bldg., 101 Twelfth Ave.

Chapter X

Ground-Water Chemistry and Diagenetic Reactions in Tertiary Sandstones of the Green River and Wasatch Formations, Uinta Basin, Utah

By RICHARD B. WANTY, JANET K. PITMAN, and THOMAS D. FOUCH

A multidisciplinary approach to research studies of sedimentary rocks and their constituents and the evolution of sedimentary basins, both ancient and modern

U.S. GEOLOGICAL SURVEY BULLETIN 1787

EVOLUTION OF SEDIMENTARY BASINS—UINTA AND PICEANCE BASINS

U.S. DEPARTMENT OF THE INTERIOR
MANUEL LUJAN, JR., Secretary

U.S. GEOLOGICAL SURVEY
Dallas L. Peck, Director

UNITED STATES GOVERNMENT PRINTING OFFICE: 1991

For sale by the
Books and Open-File Reports Section
U.S. Geological Survey
Federal Center
Box 25425
Denver, CO 80225

Library of Congress Cataloging-in-Publication Data

Wanty, Richard B.
Ground-water chemistry and diagenetic reactions in Tertiary sandstones of the Green River and Wasatch Formations, Uinta Basin, Utah : a multidisciplinary approach to research studies of sedimentary rocks and their constituents and the evolution of sedimentary basins, both ancient and modern / by Richard B. Wanty, Janet K. Pitman, and Thomas D. Fouch.
p. cm. — (U.S. Geological Survey Bulletin ; 1787) (Evolution of sedimentary basins—Uinta and Piceance basins ; ch.)
Includes bibliographical references.
1. Water, Underground—Uinta Basin (Utah and Colo.) 2. Sandstone—Uinta Basin (Utah and Colo.) 3. Water chemistry. 4. Green River Formation. 5. Wasatch Formation. I. Pitman, Janet K. II. Fouch, Thomas D. III. Title. IV. Series. V. Series: Evolution of sedimentary basins—Uinta and Piceance basins ; ch.
QE75.B9 no. 1787–X
[GB1027.U38]
557.3 s—dc20 91–25812
[552'.5] CIP

CONTENTS

FIGURES

TABLES

Ground-Water Chemistry and Diagenetic Reactions in Tertiary Sandstones of the Green River and Wasatch Formations, Uinta Basin, Utah,

By Richard B. Wanty, Janet K. Pitman, *and* Thomas D. Fouch

Abstract

An integrated study of ground-water chemistry and aquifer petrology reveals close correspondence between the chemical evolution of ground water and observed authigenic mineral assemblages. In recharge areas, authigenic kaolinite is observed in the rocks, and ground-water compositions plot within the stability field for kaolinite in a variety of activity-activity diagrams. Feldspar is dissolved from the updip rocks, also in accordance with thermodynamic predictions from the water chemistry. In down-gradient reaches of the flow system, authigenic clay, including smectite and illite-smectite, is present and feldspar destruction still prevalent. Near discharge areas, feldspar may be stable, although authigenic feldspar is not common. Throughout the basin, authigenic calcite and dolomite commonly replace detrital feldspar grains. Precipitation of carbonate minerals probably is driven by an increase in pH and by release of calcium associated with feldspar dissolution. Chalcedony, rather than quartz, probably is the silicate phase controlling dissolved silica levels. The good agreement between the petrographic relationships and the present-day ground-water chemistry suggests either that the observed authigenic mineral assemblages are still forming or that the ground water has had sufficient time to approach equilibrium with respect to the assemblage.

INTRODUCTION

Although numerous workers have examined diagenetic changes in sandstones or basinwide changes in water chemistry, few of them have integrated water and rock data. In a study of Tertiary sandstones in the Kettleman North Dome in California, Merino (1975a, b) found that diagenetic minerals and water were in chemical equilibrium. When plotted on activity-activity diagrams showing stability fields for major silicate minerals, the water compositions were within stability fields for minerals observed to be present as authigenic phases in the sandstones. In a similar study, Lee (1985) found that water chemistry in Upper Cretaceous aquifers in the Mississippi embayment of northern Mississippi and Alabama followed a systematic progression that could be related to attainment of chemical equilibrium with varied diagenetic mineral assemblages along a flow path (Hanor and McManus, 1988). Further, Lee (1985) used carbon isotopic ratios to infer sources and sinks of dissolved inorganic carbon in the waters.

The studies described above show the validity of using theoretical models to understand natural systems, and they serve as appropriate examples for our study of ground waters in Tertiary sandstones of the Green River and Wasatch Formations in the Uinta basin of northeastern Utah (fig. 1). We calculated mineral assemblages that are in equilibrium with the observed waters and compared calculated and observed assemblages to test how well mineral-solution equilibria characterize the processes of water-rock interaction in the basin.

Geologic Setting

The Tertiary Green River and Wasatch Formations in the Uinta basin are made up of lacustrine and fluvial sublitharenite, litharenite, feldspathic litharenite, and lithic arkose deposited along the margin of ancient lake Uinta during the Paleocene and Eocene. This large lake complex developed and reached its greatest areal and volumetric extent during the early Eocene to early Oligocene(?). The

Manuscript approved for publication May 21, 1991.

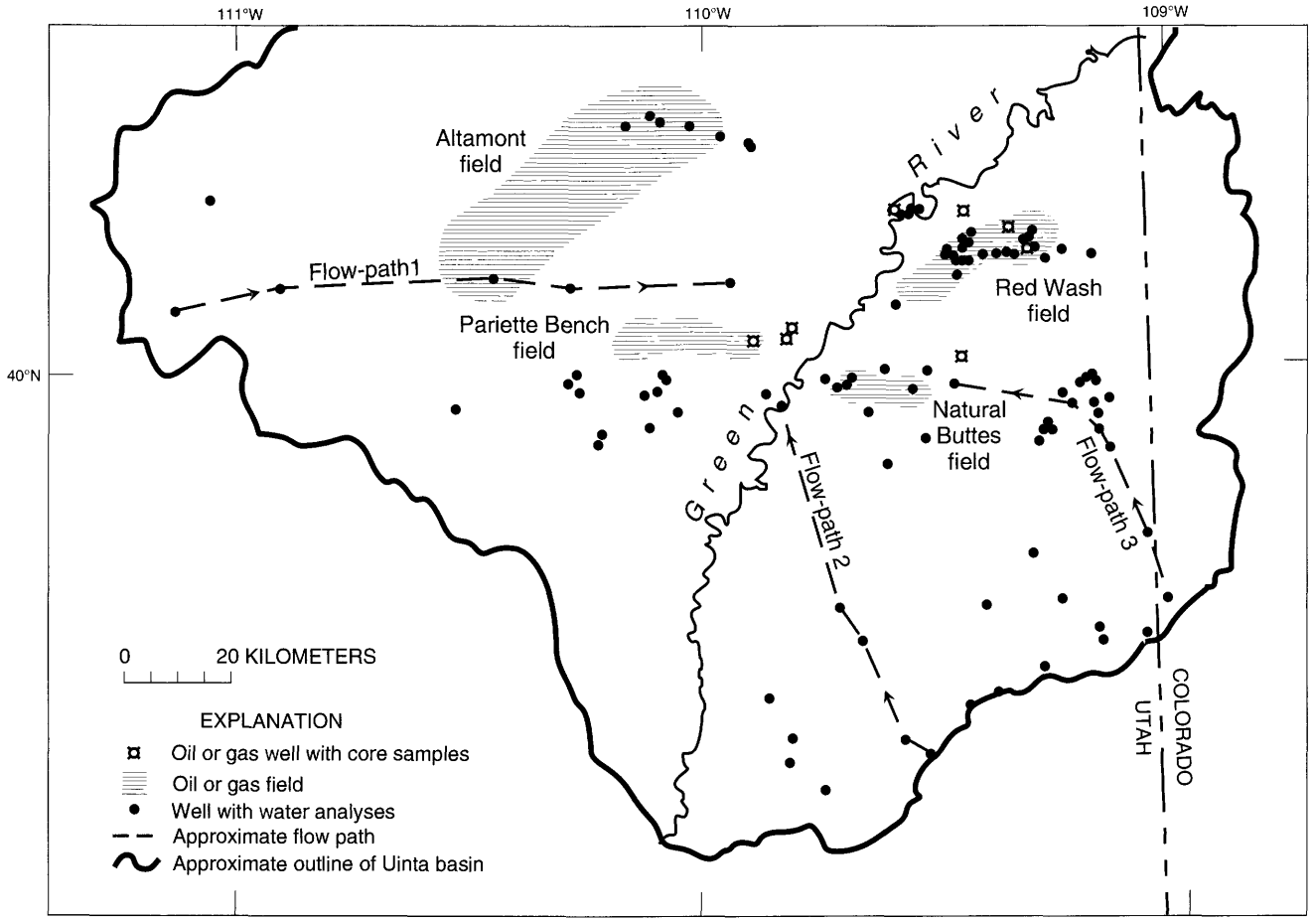

Figure 1. Map showing the locations of wells from which water or core samples were taken, Uinta basin, Utah. All water analyses are from literature sources given in the appendix. Flow-paths 1, 2, and 3 were chosen based on the hydrological model of J.D. Bredehoeft (1990, written commun.). The locations of major oil- or gas-producing fields also are shown.

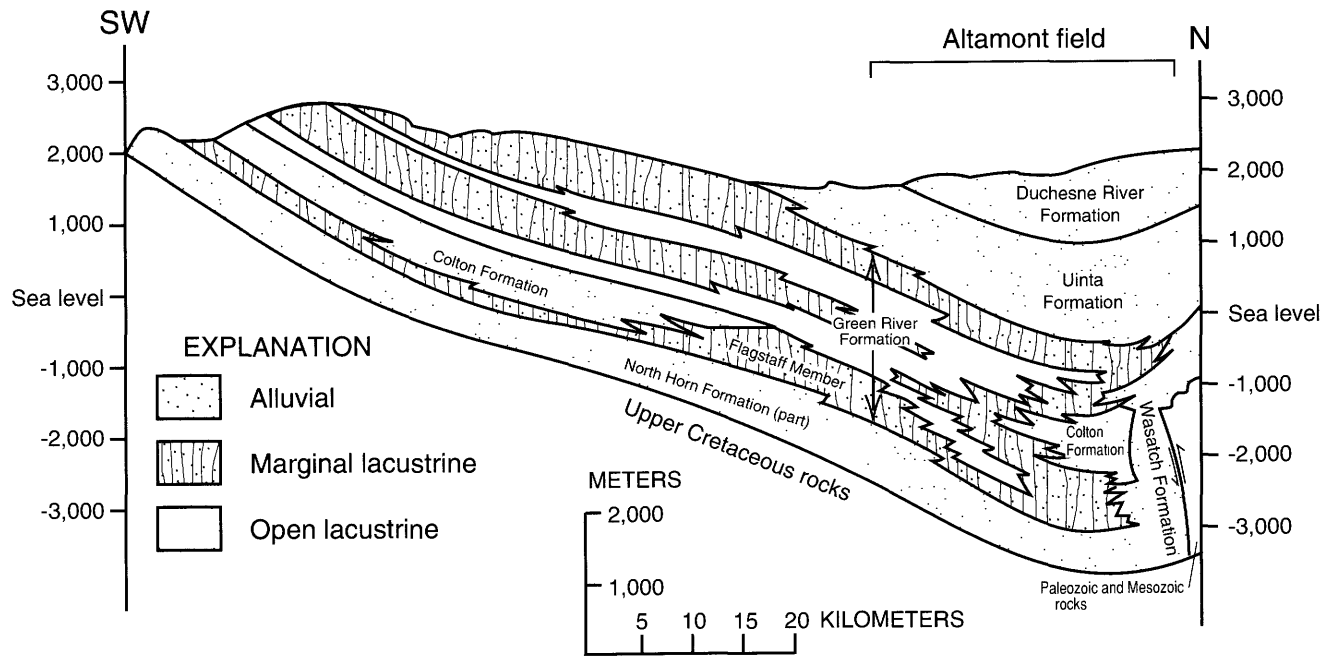

Figure 2. Lithologic cross section through the central part of the Uinta basin from southwest to north. Modified from Fouch (1975).

thickest fluvial and lacustrine sequence was deposited near the present-day Altamont oil field south of the uplifted flank of the Uinta Mountains along the central part of the axis of the Uinta basin (fig. 2). In this area, more than 3,000 m of Paleocene and Eocene lacustrine rocks are preserved, including more than 1,200 m of fine-grained kerogenous carbonate and mudstone units, including oil shale, that formed during the middle and late Eocene (46–42 Ma).

Mineral composition of rocks in the Uinta basin is related to the geographic location of source terrane (Ryder and others, 1976; Franczyk and others, 1989). In the northern part of the basin, including the areas of the Altamont and Red Wash fields, sediments were derived from granitic source rocks in the Uinta Mountains to the north. In contrast, sediments in the southern half of the basin, including the areas of the Natural Buttes and Pariette Bench fields, were derived from feldspathic- and lithic-rich rocks in Laramide uplifts to the south. The resulting distinct petrofacies experienced different diagenetic histories and consequently display different authigenic mineral assemblages. Our study deals primarily with the feldspathic- and lithic-rich rocks in the central and southern parts of the basin.

The results of this study may be applied to understanding the development or occlusion of porosity in oil- and gas-bearing strata of the Uinta basin. Oil-producing reservoirs in the Red Wash and Altamont fields include marginal-lacustrine fluvial and lacustrine sandstones that formed along the lake's northern margin. Open-lacustrine turbidites also yield oil at Altamont. Lower deltaic plain units and low-permeability sandstones, encased in redbeds, on the south flank of the basin in the Natural Buttes field and nearby areas produce gas.

Well Locations, Flow Paths, and Ground-Water Analyses

Water-chemical analyses were collected from the literature (Price and Miller, 1975; Hood and others, 1976; Conroy and Fields, 1977) and screened for completeness and accuracy. They were all evaluated according to following criteria: (1) analyses had to be reasonably complete, including measurements for pH, temperature (or depth), and major cations and anions; (2) analyses had to be charge balanced to within ±10 percent; and (3) the geologic formation producing the water had to be identified. Approximately 15 percent of the available analyses met these criteria, resulting in a total of 201 analyses. The appendix contains the unique field-identification numbers of these analyses and the sample collection dates. The full analyses can be obtained by consulting the references cited above.

Because our study is based on previously reported analyses, several limitations are imposed on data interpretation. For the most part, analytical results are limited to the major cations and anions (Ca, Mg, Na, K, ΣCO_3, Cl, and SO_4) and pH. In some cases, analytical results are reported for other elements, including silica and iron. The use of analytical results from several literature sources introduces additional uncertainty caused by possible variations in sampling protocol and technique, equipment used, and so forth, the details of which are not adequately described in the cited reports. All analyses include measurements of pH, but it is unclear whether the pH reported is at the formation-water temperature or surface temperature. All modeling in this study was performed assuming the former. The uncertainty introduced by this assumption is greatest for water samples having temperatures greater than about 30°C; that is, those collected from depths greater than about 700 m. In light of these limitations in the data set, conclusions based on individual samples are de-emphasized; rather, the data are examined with regard to describing the general trends of ground-water chemical evolution.

The present-day potentiometric surface for the middle of the Green River and Wasatch Formations in the basin is shown in figure 3 (J.D. Bredehoeft, U.S. Geological Survey, 1990, written commun.). Potentiometric highs (recharge areas) are around the perimeter of the basin, and lows (discharge areas) are along the Green River, which cuts across the basin from northeast to southwest. The three flow paths shown in figure 1 were constructed using the results of this hydrologic model. Water-rock reactions are modeled along these flow paths, from recharge areas along the basin margins to discharge areas.

The map of the Uinta basin (fig. 1) shows the locations of major oil fields in the basin as well as the locations of oil or gas wells from which core samples were collected for the petrographic, mineralogic, and isotopic parts of this study.

RESULTS

Petrography and Paragenesis

The feldspathic-lithic petrofacies that characterizes Tertiary sandstones in the southern part of the Uinta basin has been diagenetically modified by authigenic cements and by framework-grain replacement and dissolution. Of these processes, cementation and dissolution reactions have had the greatest effect on oil- and gas-reservoir quality. The extent of alteration within a sandstone sequence is highly variable and reflects the diverse compositional varieties of feldspar. This variation can account for differences in reservoir quality in rocks of the same age and origin at different locations. The paragenetic sequence of mineral alteration (fig. 4) consists of (1) minor silica cementation,

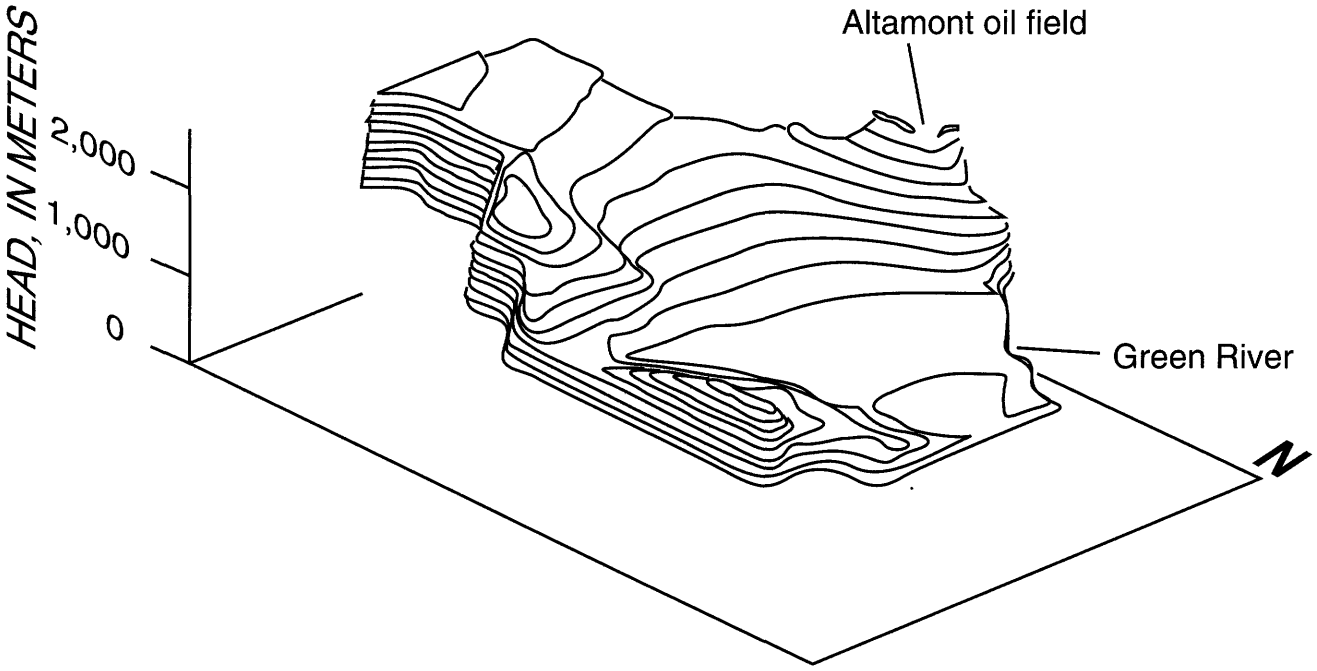

Figure 3. Plot of the potentiometric surface for the Wasatch and Green River Formations in the Uinta basin. Modified from J..D. Bredehoeft (1990, written commun.).

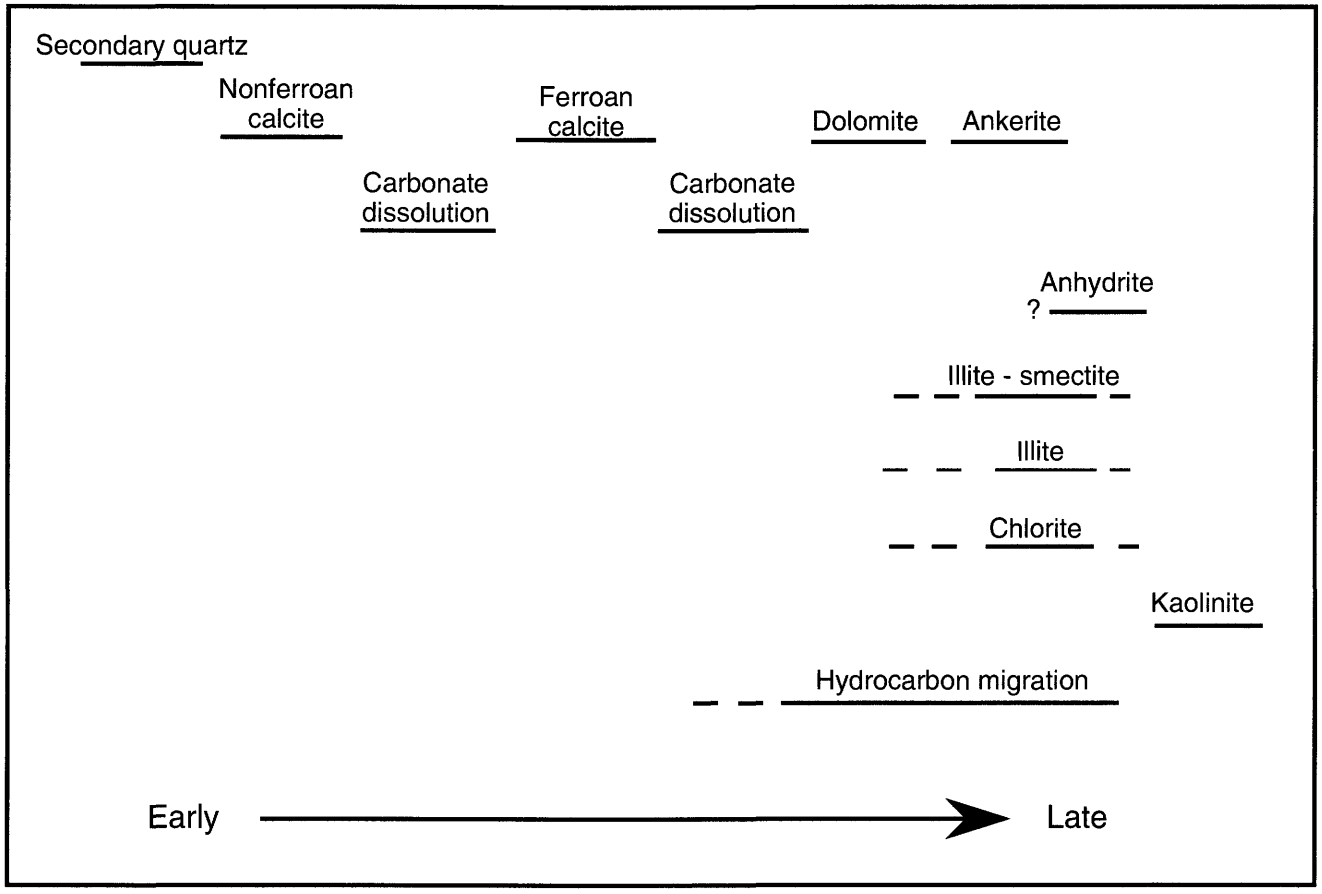

Figure 4. Generalized paragenetic sequence for sandstones of the Green River Formation in the southern half of the Uinta basin.

(2) multiple generations of carbonate precipitation and dissolution, (3) local anhydrite and barite cementation, and (4) authigenic clay mineral development. A detailed description of the various authigenic phases is given in Pitman, Fouch, and Goldhaber (1982) and Pitman, Anders, and others (1986).

Minor secondary quartz is present in some Tertiary sandstones generally as anhedral to euhedral overgrowths. Sutured grain contacts or other evidence of pressure solution were not observed. Except for the euhedral overgrowths, which are sparse, most secondary quartz overgrowths probably formed along with the detrital grains in the sediment source area and were transported to the site of sedimentation.

The sandstones have been modified by a complex carbonate mineral assemblage composed of ferroan calcite and lesser nonferroan calcite, dolomite, and ferroan dolomite. Multiple episodes of calcite precipitation can be distinguished on the basis of trace-element concentrations. For example, early calcite is iron poor (Fe:Ca atomic ratio <0.05), but later calcite is iron rich (Fe:Ca atomic ratio as high as 0.2). Ferroan calcite is common in sandstones throughout the southern part of the basin, whereas ankerite is abundant only in the central part of the basin at the Pariette Bench field. The amount and distribution of authigenic carbonate within and between beds may be widespread or localized depending on the depositional environment. Iron-free calcite, the earliest carbonate phase to precipitate, is present as relict grains and cement surrounded by optically continuous ferroan calcite. The embayed texture of nonferroan calcite relicts suggests that this carbonate phase was affected by dissolution early in the diagenetic history. Most calcite is a fine- to coarse-crystalline ferroan variety that formed during later stages of diagenesis. Typically, it partly to completely replaces feldspar grains and rock fragments and occludes pores. In sandstones that probably had high initial porosity and permeability, ferroan calcite is a pervasive cement. Framework grains enclosed in the cement typically are angular, show little or no alteration, and are not in contact with one another. The "rind" of ferroan calcite cement probably protected the grains from later alteration by chemically active pore fluids. In many sandstones calcite and possibly other mineral cements may have been widespread. Feldspar grains and lithic fragments having embayed margins, calcite relicts in pores, and calcite along cleavage planes in feldspar grains suggest that an episode of leaching occurred during late-stage diagenesis.

Calcite dissolution features in Tertiary sandstones reflect multiple episodes of leaching during different times in the burial history. Thermal maturation of coeval, deeply buried organic-rich rocks at the Altamont field in the northern part of the basin and subsequent oil migration southward to the Pariette Bench field may have yielded CO_2 and organic acids to pore fluids. These compounds could have promoted carbonate dissolution. There is no evidence that oil migration affected Tertiary strata at the Natural Buttes field, but the presence of thermogenic gas in the thermally immature rocks of the field could signal the presence of organic acids. More likely, carbonate dissolution occurred when meteoric waters infiltrated these rocks during a period of erosion.

Similar to calcite, dolomite is present as isolated grains and small patches of cement; however, authigenic dolomite is difficult to differentiate from detrital dolomite because the two phases are complexly intergrown. Where authigenic dolomite is abundant, it is as an anhedral pore-fill and replacement cement that probably formed relatively early in the burial history. Ferroan dolomite is present both as optically continuous rims on detrital dolomite grains and as discrete rhombs that commonly have coalesced to form a cement. There is no evidence of leaching in any of the rocks studied. Most ferroan dolomite probably formed in the source area and was introduced with other detrital grains, although a small fraction clearly precipitated during late-stage diagenesis.

The complex carbonate mineral assemblage indicates that carbonate- and bicarbonate-charged waters of variable chemical composition migrated intermittently through the sandstone sequence during burial, resulting in multiple cycles of carbonate precipitation and dissolution. A similar interpretation is supported by stable isotope analyses of end-member carbonate cements in the Natural Buttes field. Widely variable calcite $\delta^{13}C$ values (about –1 to –9 per mil relative to PDB) suggest that multiple sources of carbon were added to the carbon reservoir through time. Heavy carbon values (>–2 per mil relative to PDB) probably result from recycled dissolved marine carbonate grains, whereas lighter values (<–2 per mil relative to PDB) can be attributed to the decomposition of organic material. Carbonate $\delta^{18}O$ values also vary significantly (about –6 to –13 per mil relative to PDB). Heavier values in more deeply buried Cretaceous rocks suggest that temperature was not the dominant controlling factor. Rather, the trend toward heavier oxygen isotopic values is interpreted to record progressive reaction between meteoric waters and silicate minerals along a basinward flow path.

Authigenic anhydrite and barite are present only in sandstones at the Natural Buttes field. Both minerals preferentially replace carbonate cement and framework grains such as feldspar, thus they probably formed relatively late in the diagenetic history. Preliminary sulfur isotope data for anhydrite cement in Tertiary sandstones at the Natural Buttes field show isotopically heavy values averaging about +30 per mil relative to CDT. These values are similar to those reported for organic and pyrite sulfur in younger kerogenous beds of the Green River Formation (Harrison and Thode, 1958; Mauger, 1972; Cole and Picard, 1981;

Table 1. Chemical analyses for samples that fall along flow-paths 1, 2, and 3

[Depth in meters; temperature in °C; all chemical constituents, including total dissolved solids (TDS), in milligrams per liter. Leader (—) indicates no value reported]

	Avg. depth	pH	Temperature	Ca	Mg	Na	K	HCO_3	CO_3	SO_4	Cl	SiO_2	TDS
Flow-path 1													
GR-142	0	7.6	8.0	56	37	14	1.4	316	—	74	3.4	25	527
GR-141	360	8.9	17.9	10	13	210	—	426	—	120	12	—	790
GR-140	2,320	8.7	65.3	20	16	3,020	24	3,220	—	72	2,560	—	8,900
GR-71	2,320	8.7	65.3	20	16	3,020	24	3,220	230	72	2,560	—	9,160
GR-69	2,140	8.5	61.0	16	7	4,300	—	1,730	250	79	5,300	—	11,700
GR-67	1,480	8.3	44.8	17	—	23,800	150	4,360	280	102	34,000	—	62,700
GR-68	1,900	8.4	55.0	22	20	17,300	170	2,090	200	580	25,000	—	45,400
Flow-path 2													
GR-226	0	7.5	7	77	26	27	0.8	303	—	100	2.2	23	559
GR-225	0	8.4	11	48	20	33	0.9	268	—	44	3.5	18	435
GR-215	0	7.9	11	65	17	27	0.4	250	—	52	14	14	439
GR-111	690	8.7	25.8	10	7	274	13	380	—	290	32	—	1,000
GR-49	1,480	7.9	44.8	2,060	270	23,600	—	425	—	3,580	38,000	—	68,000
GR-51	1,350	8.4	41.7	590	310	28,700	—	427	36	11,900	37,200	—	79,000
GR-52	3,900	8.1	43.4	990	270	26,800	—	878	—	2,800	41,300	—	73,000
GR-53	1550	8.1	46.6	1,920	360	21,600	—	647	—	3,700	34,600	—	62,800

Flow-path 3

	Avg. depth	pH	Temperature	Ca	Mg	Na	K	HCO_3	SO_4	Cl	F
GR-229	0	7.2	8.5	53	27	12	0.7	267	47	2.8	0.3
GR-212	0	7.7	10	110	170	1,200	7.7	556	2,900	65	0.5
GR-210	10	7.8	10.5	76	150	870	4	540	1,600	390	6.6
GR-211	10	7.4	10.5	64	150	890	3.1	545	1,900	190	6.2
GR-208	3	8	9.5	150	180	1,000	8.9	530	2,500	65	1.9
GR-209	3	7.6	9	130	180	970	6.9	564	2,500	59	2.1
GR-196	185	8.4	14.5	2.4	3.7	640	1.8	880	350	170	2.6
GR-147	494	8.3	21.5	2.1	1.2	2,400	11	779	140	3,200	
GR-148	508	8.5	22	4	1	3,100	11	2,260	100	3,300	25
GR-144	327	8.5	17	1.1	0.5	3,400	11	5,100	58	1,700	120

	SiO_2	S^{2-}	Fe	Mn	B	Al	Sr	V	U	TDS
GR-229	17	0.1	0.02	—	0.02	—	0.5	—	—	427
GR-212	8.3	0.1	0.05	—	0.13	—	3.4	—	—	5,020
GR-210	19	180	0.04	0.01	7		2.9	0.0031	0.0069	3,850
GR-211	19	180	0.06	0.03	7.9	0.01	2.9	0.017	0.0002	3,960
GR-208	13	0.1	0.06	0.06	4.7	—	3	0.0005	0.02	4,460
GR-209	12	0.2	0.32	0.06	1.8	—	3.4	0.0021	0.022	4,430
GR-196	15	120	0.1	0.02	2	0.03	0.46	0.001	0.0008	2,190
GR-147	15	6.5	0.09	—	20	—	0.81	—	—	6,580
GR-148	15	6.7	0.06	—	21	0.02	0.97	—	—	8,850
GR-144	11	0.5	0.05	—	33	—	0.34	—	—	10,400

Tuttle, 1988). Fluids expelled from tongues of organic-rich shale may have contained reduced sulfur that was later transported to Wasatch Formation strata where the sulfur was oxidized to sulfate.

Authigenic kaolinite, chlorite, illite, and illite-smectite commonly are present together in various amounts at the Natural Buttes field, but at the Pariette Bench field, more central in the basin, kaolinite is absent from this assemblage. Corrensite, a regularly interstratified illite-chlorite, also was detected in small amounts at the Natural Buttes field. Corrensite is present as a network of interconnected platelets oriented perpendicular to grain surfaces. Kaolinite generally is present as well-crystallized booklets in secondary intergranular pores that commonly

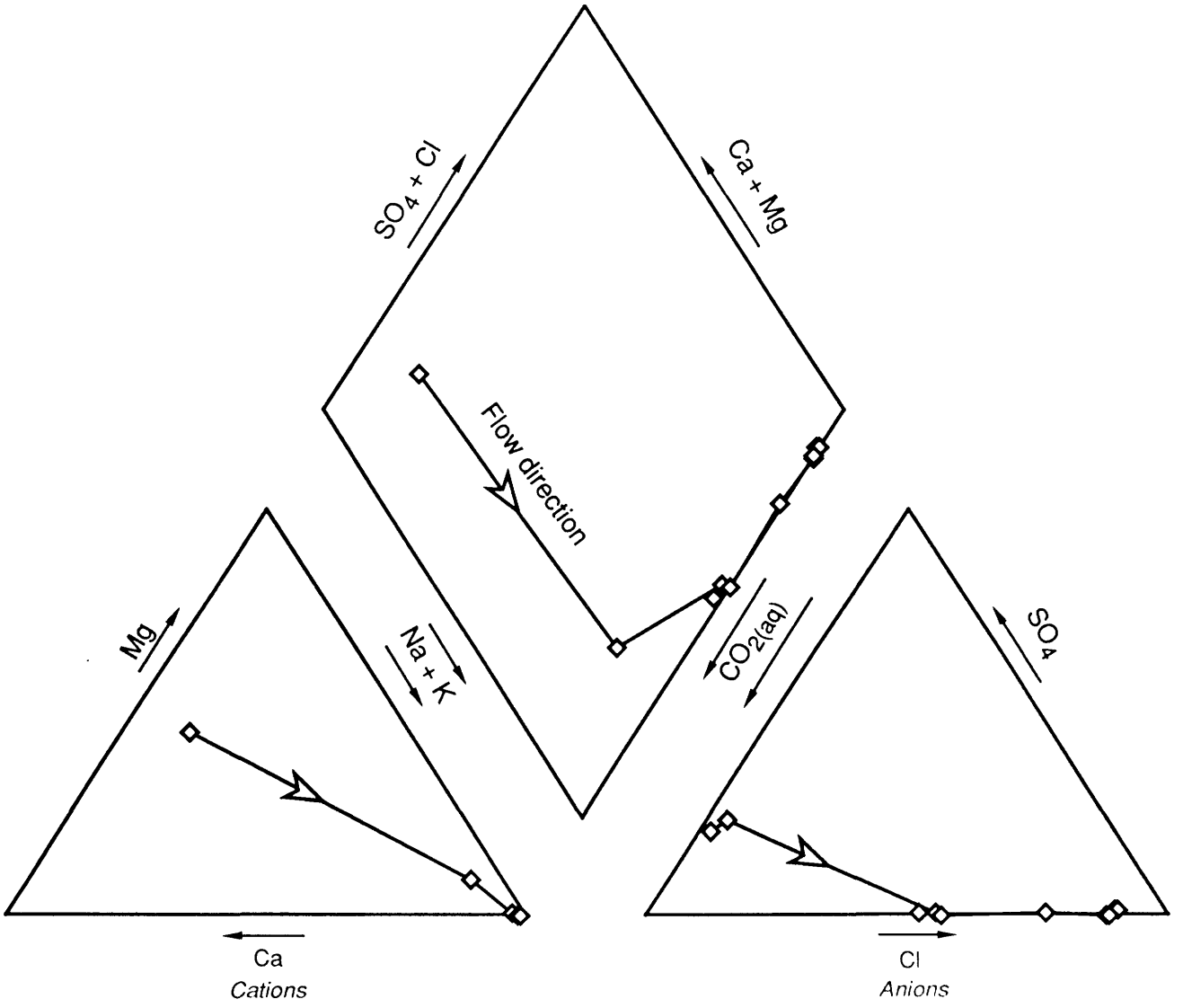

Figure 5. Piper diagram of water samples along flow-path 1 in the western half of the Uinta basin. The triangular fields show normalized percentages of the equivalents per million of cations or anions.

are lined with fibrous illite or platelets of chlorite. Textural relations suggest that the suite of authigenic clay minerals formed over a long time span after carbonate dissolution. Illite, illite-smectite, and chlorite probably formed when the rocks were at or near maximum burial, whereas kaolinite precipitation most likely is related to an influx of meteoric water associated with late-stage uplift and erosion.

Ground-Water Chemistry

The chemistry of ground water evolves along the flow paths in a systematic manner. Chemical analyses are given in table 1 for samples that plot along the three flow paths shown in figure 1. From recharge zones, the waters show increasing total dissolved solids (TDS) contents as they move down gradient. Low-TDS waters are Ca-Mg-HCO_3 dominated, whereas high-TDS waters are Na-Cl dominated. Waters in the basin are typically low in sulfate. Ground-water chemical evolution is conveniently summarized in Piper diagrams (figs. 5–7). Profile plots in figures 8–10 demonstrate the increase in TDS, as well as the increase in Na:Ca and Cl:CO_3 ratios along the three flow paths.

DISCUSSION

The interpretation of ground-water chemical changes described here is based on the application of thermodynamic models that assume chemical equilibrium. Therefore, further limitations are introduced in addition to those described earlier that relate to the use of previously

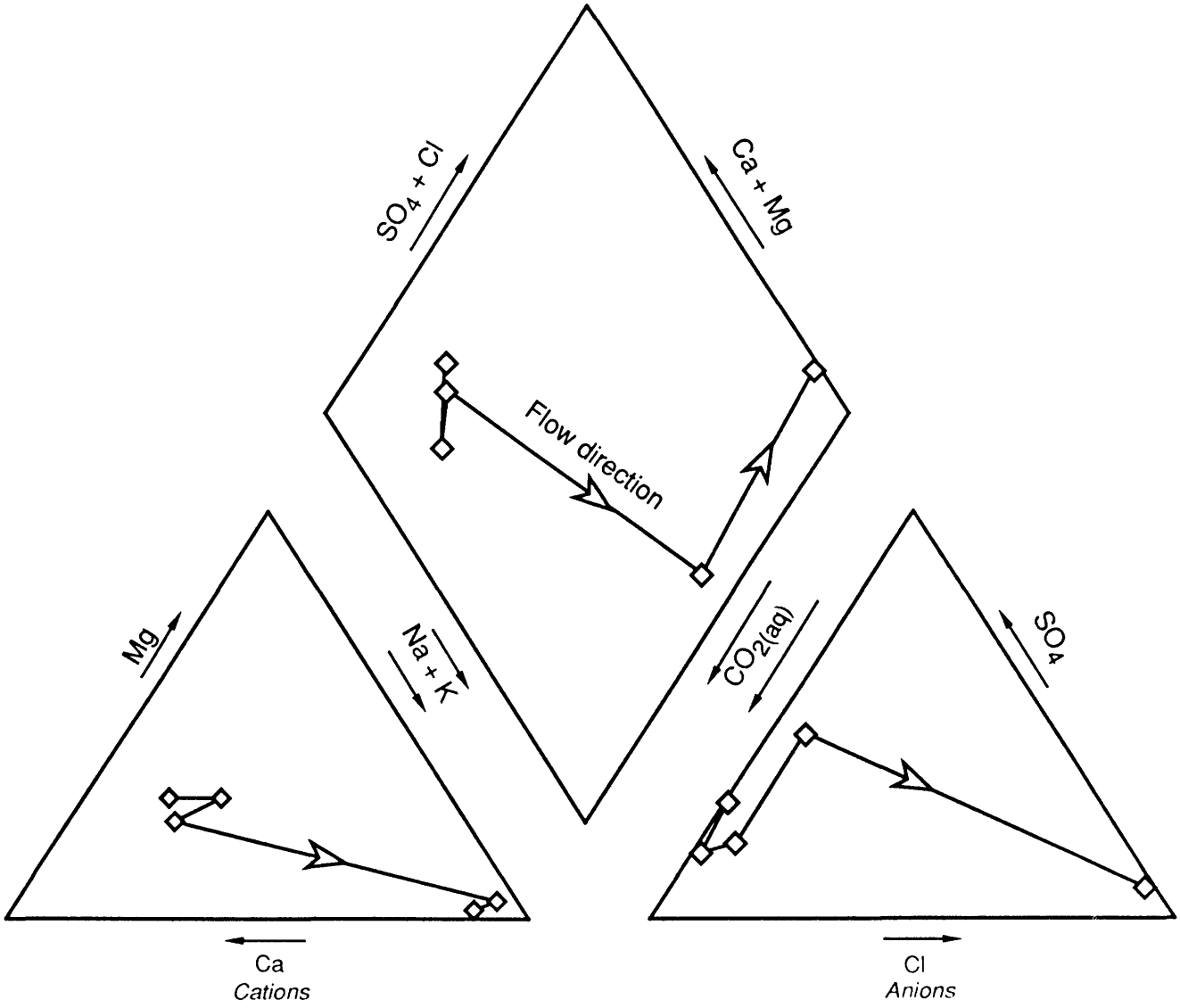

Figure 6. Piper diagram of water samples along flow-path 2 in the southern part of the Uinta basin. The triangular fields show normalized percentages of the equivalents per million of cations or anions.

published chemical analyses. The primary limitation of thermodynamic modeling is the availability of reliable and complete thermodynamic data for calculation of equilibrium constants. In many instances, thermodynamic data may be available for 25 °C, but the lack of enthalpy values makes temperature corrections or extrapolations uncertain. In addition, complexing agents not included in the thermodynamic data base may dramatically alter the distribution of aqueous species. Kharaka and others (1988) have thoroughly discussed these types of limitations.

When modeling ground-water chemical evolution along a flow path, the choice of possible chemical reactions between water and rock is constrained by petrographic, geologic, geochemical, and other observations. Chemical evolution pathways based on these preferred reactions may be realistic but are by no means unique, a factor that must be considered when interpreting the results.

Chemical Evolution of the Ground Water

Changes in ground-water chemistry occur in response to several factors. Many of the features of the chemical evolution of the ground water can be explained in terms of mineral dissolution and precipitation reactions, as will be seen in more detail in the next section.

Along the flow paths, sample depths range from less than 30 to more than 1,500 m, and corresponding water temperatures increase from about 9 °C in springs and near-surface wells to 40–50 °C in deeper wells. The increase in solubilities (and rates of dissolution) for silicate

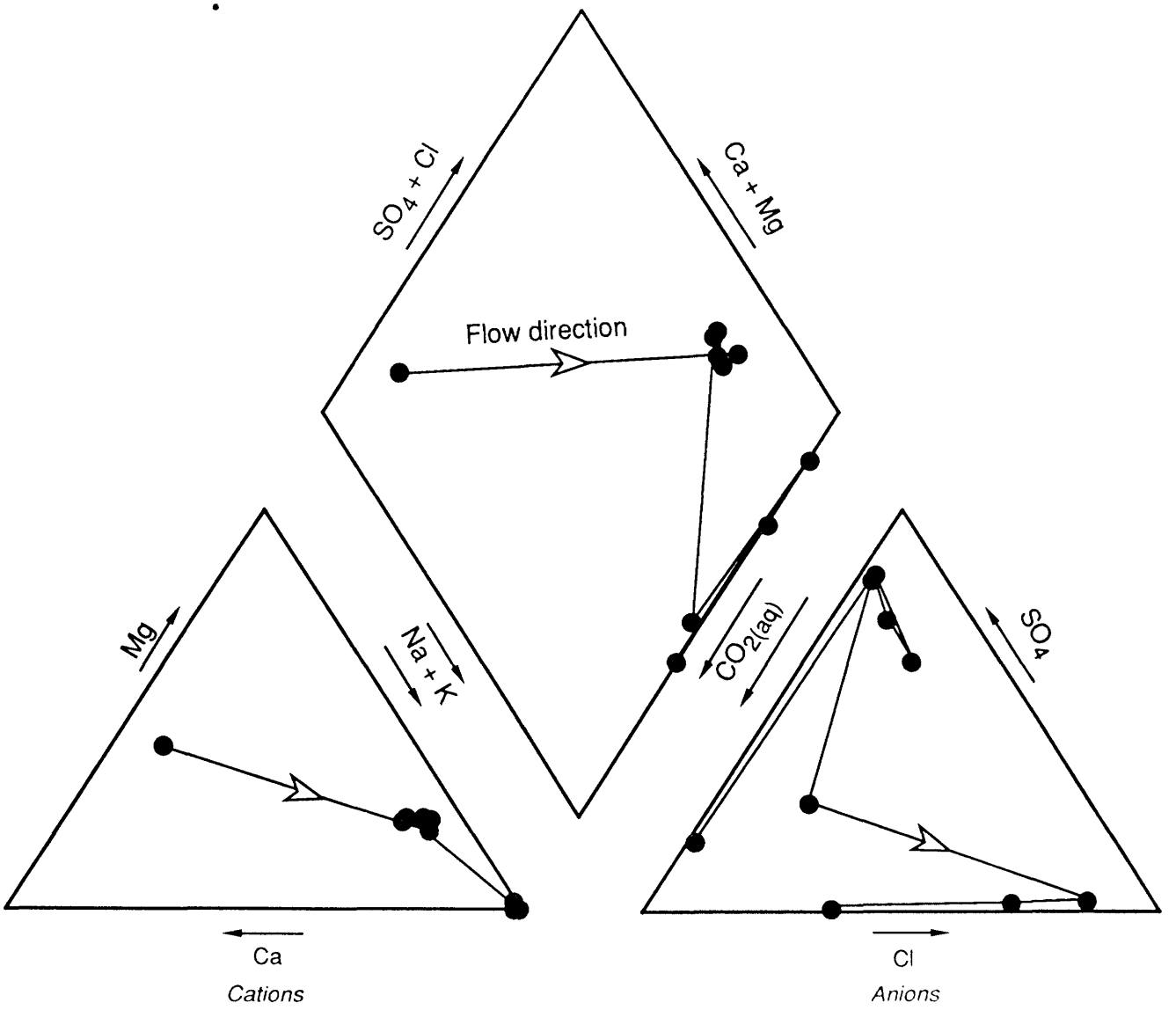

Figure 7. Piper diagram of water samples along flow-path 3 in the southeastern part of the Uinta basin. The triangular fields show normalized percentages of the equivalents per million of cations or anions.

minerals as temperature increases may contribute somewhat to the increase in concentrations of various elements with depth. Ion exchange reactions also may play a role, especially as manifested in the increase in Na:Ca ratios with distance along the flow paths. The changes in ground-water chemistry in response to these types of reactions are subtle in terms of TDS contents. As shown in figures 8–10, TDS contents increase slightly along the flow path until the deeper parts of the basin are reached, where TDS contents increase dramatically. The very high TDS levels must be due to other mechanisms such as salt dissolution, mixing with connate water, or mixing with migrated brines. These possibilities will be discussed at greater length later.

Silica Solubility

The state of saturation of the ground water with respect to silica minerals is of interest because it identifies which silica phases may be important in controlling dissolved silica concentrations. Because water samples interpreted in this study range from outcrop (spring) to deep drill-hole samples, temperatures from about 8 to more than 100 °C were encountered. The three flow paths shown in figure 1 are limited to the shallower southern part of the basin, and the maximum temperature along these flow paths is about 45 °C. Using the computer program PHREEQE (Parkhurst and others, 1980), saturation indexes (SI) were

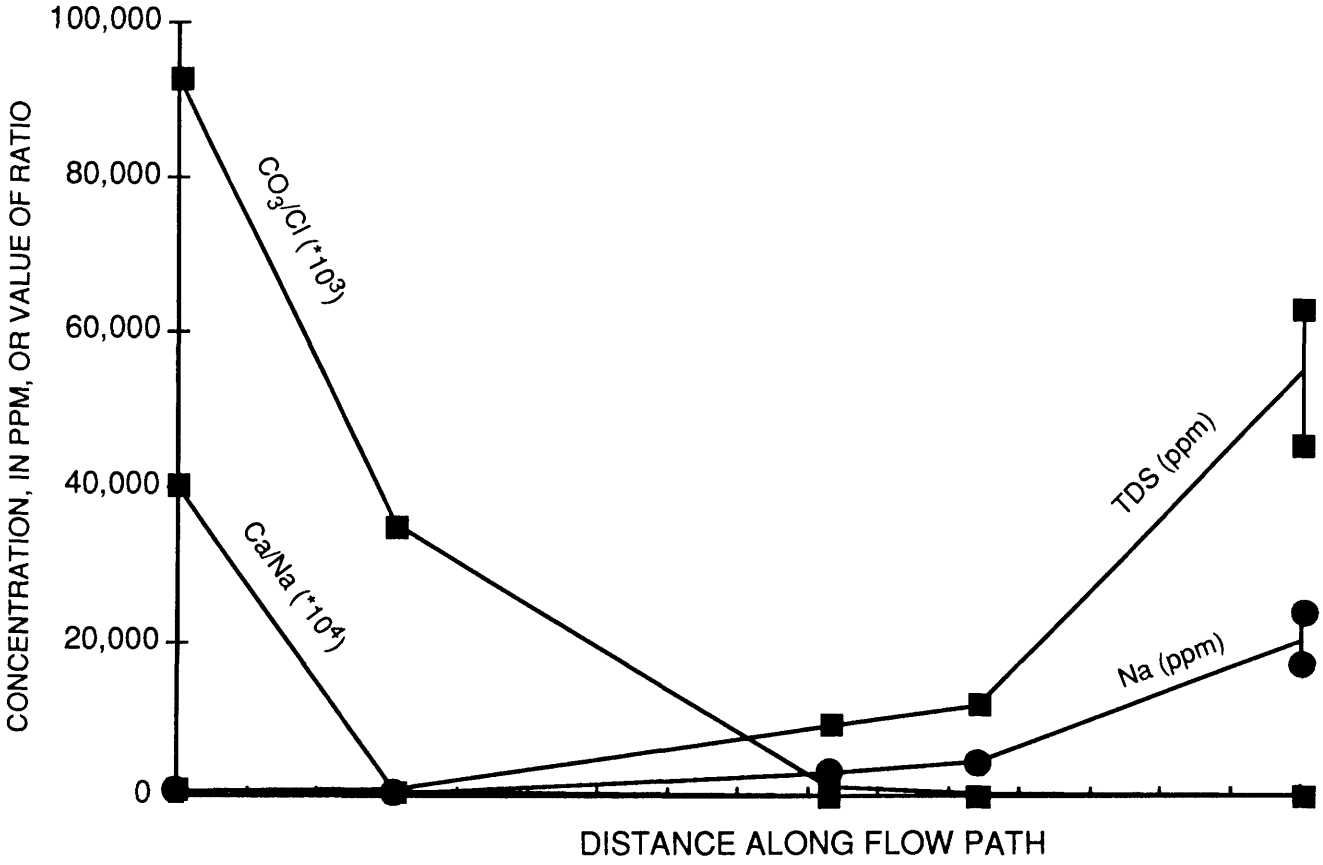

Figure 8. Profile of changes in some major ground-water chemical parameters along flow-path 1. Distance along the *x*-axis is proportional to geographic distance between wells sampled. Total length of the flow path is approximately 100 km.

calculated for chalcedony and quartz using the reaction

$$SiO_{2(s)}+2H_2O \Leftrightarrow H_4SiO_{4(aq)},$$

where $SiO_{2(s)}$ represents either chalcedony or quartz. For this reaction, the saturation index is defined as

$$SI \equiv \log_{10} \frac{a\,(H_4SiO_{4(aq)})}{a\,(H_2O)^2} \log_{10} K_T .$$

Here, a(i) denotes the observed activity of the species in parentheses, and K_T represents the appropriate equilibrium constant corrected for the temperature. Figure 11 shows histograms of SI values for the 41 samples for which silica was reported and for which the temperature was less than 45 °C. The mean SI value (±1 standard deviation) for quartz is 0.49±0.23 and for chalcedony 0.04±0.22. As shown in figure 11, chalcedony is consistently closer to an equilibrium SI value of zero than is quartz, which is generally supersaturated. These calculations suggest that the solubility of cryptocrystalline chalcedony controls silica concentrations in the shallower waters (<1,500 m) of the Uinta basin, even though macrocrystalline quartz is the thermodynamically stable phase.

Flow-Path Modeling

Chemical changes along the three flow paths shown in figure 1 were modeled using the computer programs BALANCE (Parkhurst and others, 1982), PHREEQE (Parkhurst and others, 1980), SOLMINEQ.88 (Kharaka and others, 1988), and SNORM (Bodine and Jones, 1986). PHREEQE and SOLMINEQ.88 were used to calculate saturation indexes of the ground waters and to model reaction paths. BALANCE was used at the front end of the reaction-path modeling to create general chemical models not constrained by thermodynamics. SNORM was used to examine major-salt contents of each of the water samples. Mass-transfer reactions such as dissolution or precipitation of carbonate minerals, quartz or chalcedony, and feldspar minerals were considered in the reaction-path models. Initial results provided adequate simulations of the changes in pH and alkaline-earth-element concentrations, but changes in salinity could not be adequately modeled without consideration of NaCl addition.

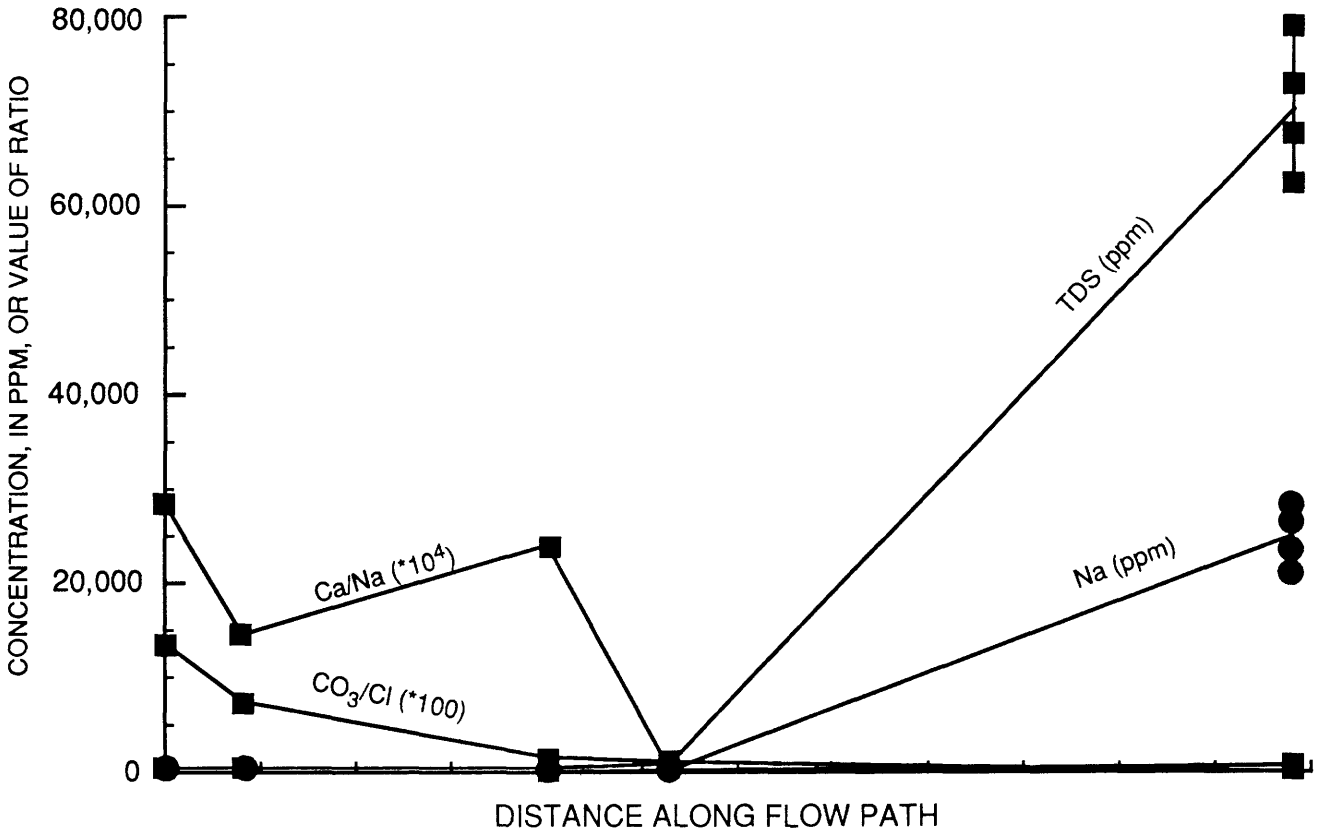

Figure 9. Profile of changes in some major ground-water chemical parameters along flow-path 2. Distance along the *x*-axis is proportional to the geographic distance between the wells sampled. Total length of the flow path is approximately 80 km.

Processes Affecting pH and Alkaline-Earth Elements

Flow-path 3 (fig. 1) was modeled in the greatest detail because it includes samples having the most complete chemical analyses. Several different simulations were run; the features of each are described in table 2. The adequacy of each model can be judged in several ways. First, the reactions included in the model should conform, as closely as possible, to observed changes in mineralogy and water chemistry throughout the basin. Second, the calculated concentrations of the major solutes at each point along the flow path should mimic observed concentrations. Third, calculated dissolution or precipitation of minerals not specifically required to react with the solution should match observed petrographic relationships.

Thermodynamic calculations of solution-mineral equilibria based on measured water compositions indicate that calcite or dolomite should dissolve in recharge areas but precipitate deeper in the basin. Carbonate-mineral precipitation is driven by the progressive dissolution of feldspar and the concomitant rise in pH. Our petrographic observations indicate that carbonate precipitation may be active in some areas of the basin not extensively affected by petroleum migration; however, generation of CO_2 during bacterial metabolism of hydrocarbons may prevent precipitation of calcite or dolomite or lead to its dissolution. To a limited extent, the increase in temperature along the flow paths aids calcite or dolomite precipitation because of the retrograde solubilities of these minerals.

Silica concentrations in the waters probably are controlled by the solubility of chalcedony or some silicate that has a solubility similar to chalcedony. For reaction-path calculations that impose a limit on dissolved silica concentrations, equilibrium between chalcedony and the ground water is assumed.

Chemical reactions occurring along the flow path were modeled as a series of mineral precipitation and dissolution reactions. The appropriate phases to be considered in these reactions were chosen by considering the location of sample compositions on activity-activity diagrams such as the one shown in figure 12. Ground water in the recharge zone is well within the stability field for kaolinite, but other ground-water samples along the flow path plot along a trend that progresses toward the albite field through the muscovite field. Petrographic studies of rock samples show that authigenic kaolinite is present in outcrop and shallow subsurface samples, whereas illite or illite-smectite is present in deeper subsurface samples. Authigenic feldspar was not observed in any samples.

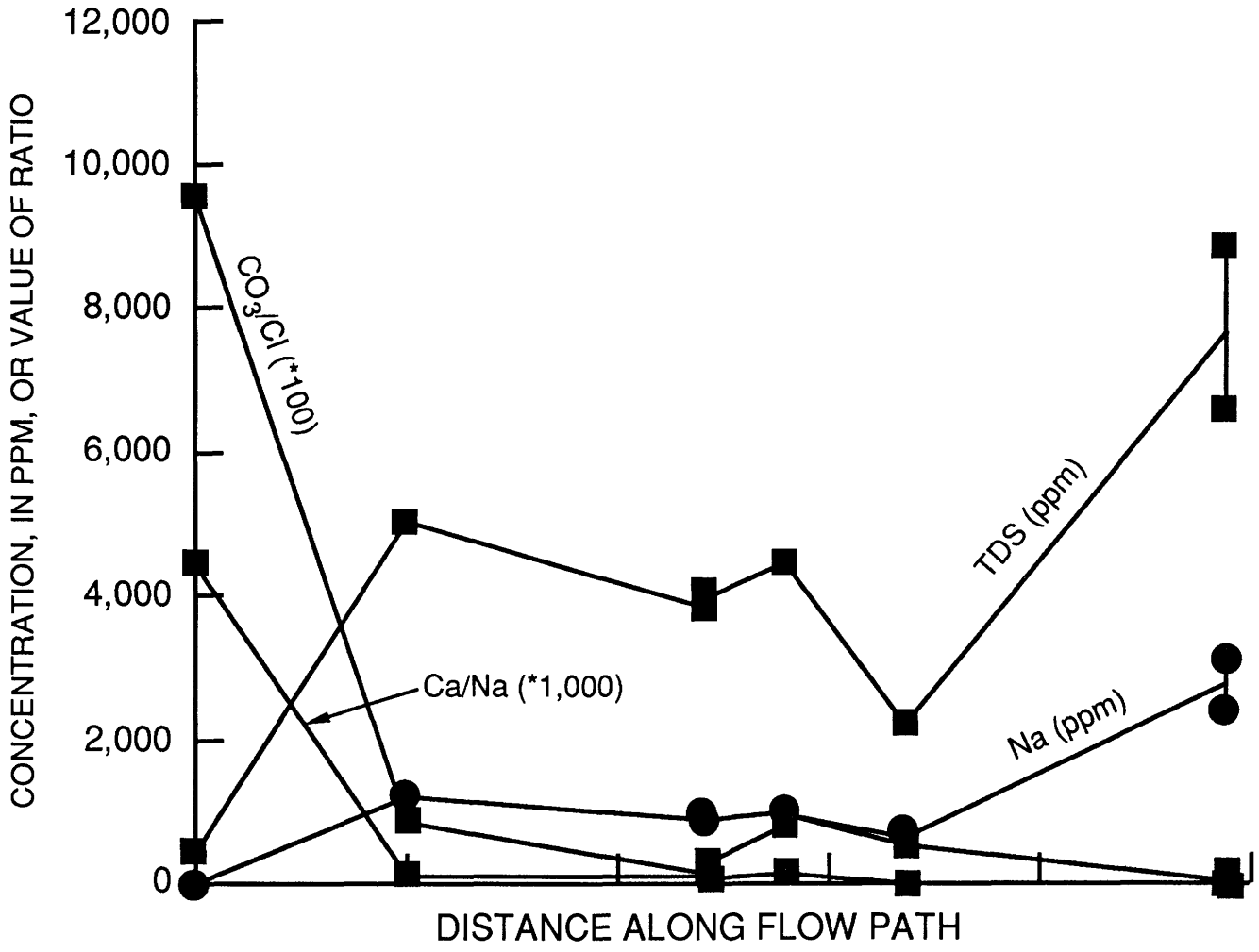

Figure 10. Profile of changes in some major ground-water chemical parameters along flow-path 3. Distance along the *x*-axis is proportional to the geographic distance between the wells sampled. Total length of the flow path is approximately 64 km.

Partial to complete destruction of detrital feldspar was observed in many of the samples. Thus, petrographic evidence of mineral dissolution and precipitation is consistent with predictions based on assumed equilibrium between minerals and coexisting ground waters.

The flow-path models had variable success in describing ground-water chemical evolution in the Green River and Wasatch interval. Models 1 and 2, for which no mineralogic control was imposed for silica, predict dissolved silica concentrations far in excess of the observed values along the flow path (fig. 13). In models 3–5, silica concentrations are limited by the solubility of chalcedony, in accordance with the earlier discussion. Models 3 and 4 give the closest fit of the observed changes when plotted on a variety of activity-activity diagrams. Silica concentrations in model 5 are somewhat higher than in models 3 and 4 because temperature was increased along the flow path from 8 to 25 °C during progress of the reaction.

Models 4 and 5 produce closer fits of the data when plotted in K^+/H^+ versus Na^+/H^+ space (fig. 14). They also more closely match observed pH values in natural samples; model 4 being slightly closer. These two models predict an authigenic mineral assemblage of kaolinite, dolomite, and chalcedony. Calcite also is predicted as part of the mineral assemblage as pH increases due to dissolution of sodium feldspar. Because of a lack of iron analyses for the water samples, the models are unable to predict the iron content of authigenic carbonate minerals. There is petrographic evidence that both ferroan and nonferroan carbonate minerals replace detrital feldspar grains, consistent with the general predictions of the model.

The types of diagenetic reactions that are consistent with the chemical evolution of waters along flow-path 3 apply equally well to flow-paths 1 and 2, although minor modifications produced closer fits of the data. The important point to be made is that a few simple diagenetic reactions can explain the major changes in ground-water chemistry throughout the basin and that these same simple diagenetic reactions are consistent with textural and mineralogical changes in the rocks.

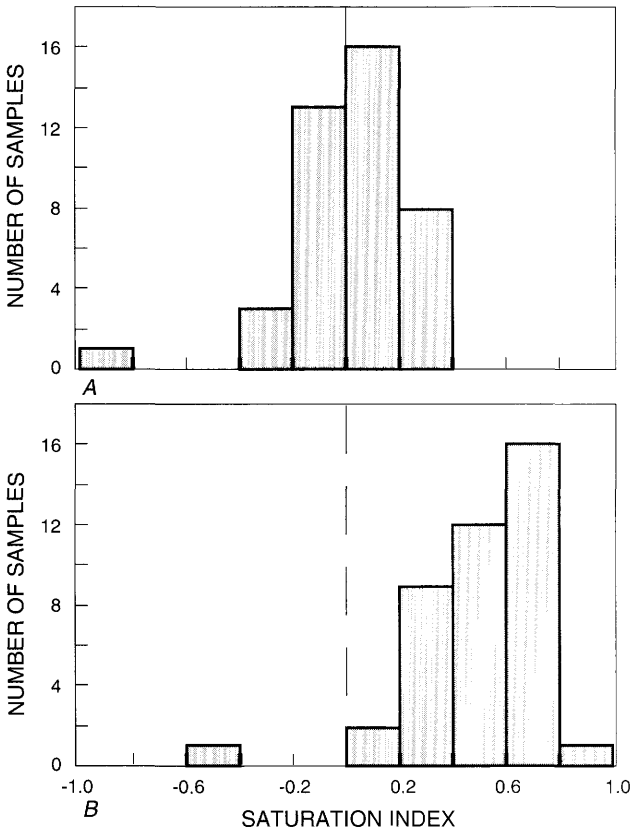

Figure 11. Histograms of calculated saturation indexes for chalcedony (*A*) and quartz (*B*) in ground-water samples interpreted in this study. Vertical dotted lines denote equilibrium. Samples having positive values of SI are supersaturated, those having negative values are undersaturated.

Processes Affecting Salinity

Models 1–5 fail to predict the dramatic increase in TDS contents in the deepest central parts of the basin (fig. 15). As seen in the Piper diagrams (figs. 5–7), the high-TDS waters contain high concentrations of sodium and chloride. One possible source of NaCl is connate water from ancient lake Uinta. M.L. Tuttle, C.A. Rice, and P.H. Briggs (U.S. Geological Survey, written commun., 1991) suggested that Soap Lake, Washington, is a possible modern analogue for ancient lake Uinta. Soap Lake has a water composition dominated by Na-CO_3-SO_4 and contains a significant amount of chloride, but the lakes that formed the Green River sediments probably had much lower sulfate concentrations because of almost complete bacterial reduction of sulfate in the water column (Tuttle, 1988). Thus, brines in ancient lake Uinta probably had a Na-CO_3-Cl character. Diagenetic evolution of this connate brine could have led to a Na-Cl character as feldspar minerals dissolved and carbonate minerals precipitated. A second source of NaCl could be upward migration of Na-Cl brines from the underlying evaporite-bearing Jurassic Arapien Shale.

Other conceptual models also may explain the high salinity of ground water in the central parts of the basin, but any conceptual model chosen must be able to explain the almost complete dominance of sodium and chloride in the ionic character of the high-TDS fluids. Therefore, the deep-basin system may be adequately modeled using a numerical model that adds halite to the solution without consideration of its origin.

Table 2. Features of models used to simulate changes in ground-water chemistry along flow-path 3

Model	Minerals held at equilibrium	Other features
1	Kaolinite	
2	Kaolinite, calcite	
3	Kaolinite, calcite, chalcedony	
4	Kaolinite, dolomite, chalcedony	
5	Kaolinite, dolomite, chalcedony	Temperature increased from 8 to 25 °C.
11	Step 1—Kaolinite, dolomite	
	Step 2—Kaolinite, dolomite, chalcedony	Dissolve sodium and potassium feldspar, add small amount of NaCl.
	Step 3—Kaolinite, dolomite, chalcedony	Add NaCl.
12	Step 1—Kaolinite, calcite, dolomite	
	Step 2—Kaolinite, calcite, dolomite, chalcedony	Dissolve sodium and potassium feldspar, add small amount of NaCl.
	Step 3—Kaolinite, calcite, dolomite, chalcedony	Add NaCl.

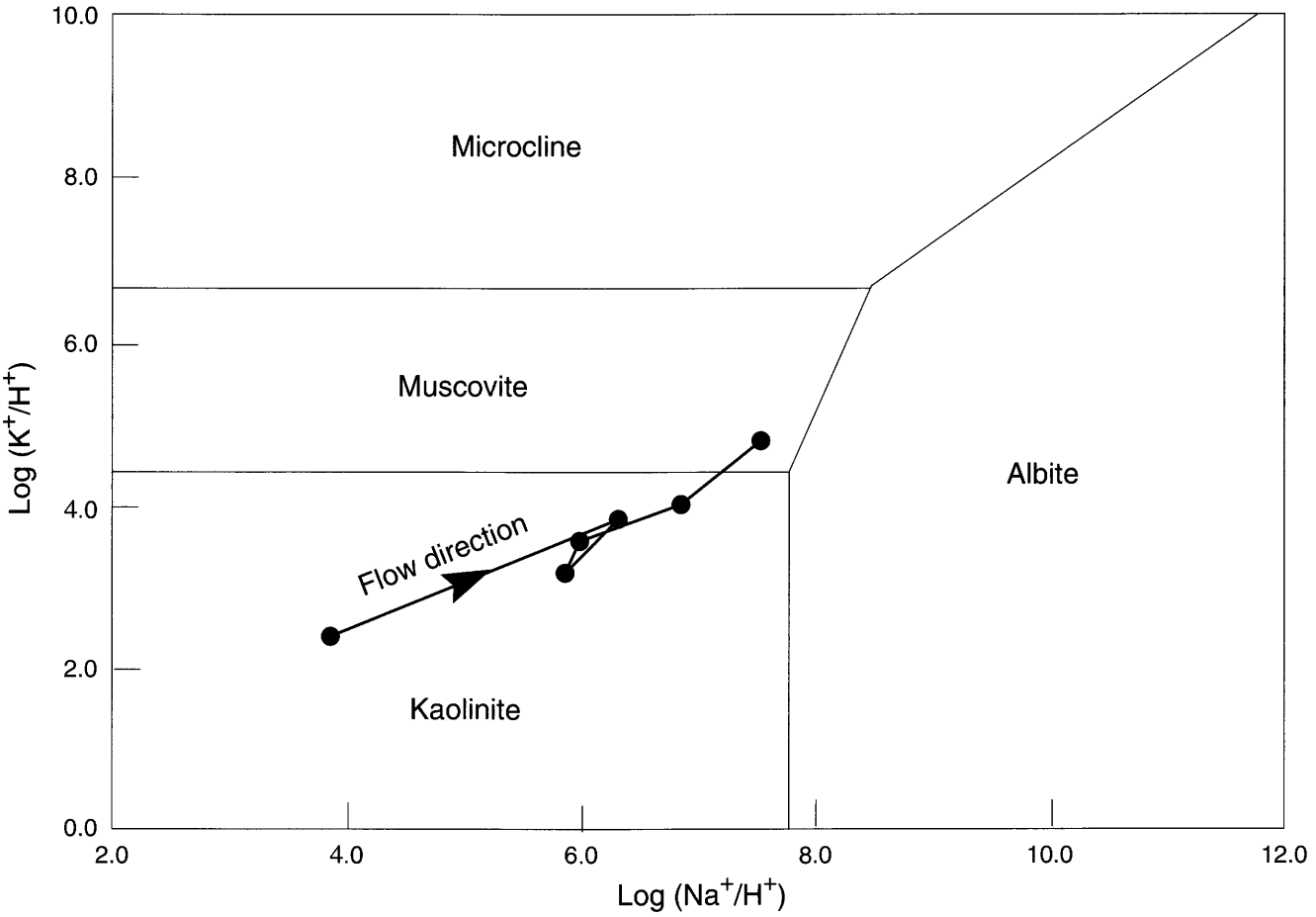

Figure 12. Evolution of ground-water chemistry along flow-path 3 in Na^+/H^+ versus K^+/H^+ space. The arrowhead depicts the direction of ground-water flow. The phase boundaries are constructed for a temperature of 25 °C. Water temperatures along flow-path 3 ranged from 8.5 to 22 °C.

Models 11 and 12, which give the closest overall fit of the data of flow-path 3, utilized three consecutive sets of reactions, with subset steps in each set (table 2). As before, the initial fluid composition was taken as the most shallow, dilute sample. The only difference between models 11 and 12 is the addition of calcite to the list of minerals constrained to be at equilibrium. Figures 16*A* and *B* show predicted variations in pH and ionic strength as compared to observed values. Figure 17 shows the model predictions in Na^+/H^+ versus K^+/H^+ space. Solution pH increases along the flow path due to dissolution of feldspar minerals, and salinity increases due to the addition of NaCl.

Models 11 and 12 require only slight modification to describe most of the ground-water chemical evolution of flow-paths 1 and 2. The major remaining problem is the higher total dissolved solids content in downdip reaches of flow-paths 1 and 2 (figs. 8–10). More NaCl must be added to adequately model flow-paths 1 and 2. In the natural system, this might correspond to a greater proportion of added brine (from whatever source) or perhaps to addition of a more concentrated brine.

CONCLUSIONS

Petrographic observations of rocks and geochemical data for coexisting waters indicate the sequence and nature of reactions that produced the authigenic phases in the Green River and Wasatch Formations in the Uinta basin. In the southern half of the basin, diagenesis took place at shallow to moderate burial depths at temperatures between 9 and 45 °C. Carbonate cement, volumetrically the most important authigenic carbonate, precipitated from meteoric waters that evolved to isotopically heavier oxygen compositions through continued reactions with silicate phases, especially feldspar. Feldspar dissolution probably occurred during maximum burial at high temperatures, and analyses of present-day ground water indicate that dissolution could still be occurring. Kaolinite is present in rocks near the basin margin and probably formed concurrent with uplift and erosion of the Colorado Plateau.

The chemistry of ground water evolves along basinward flow paths from Ca-Mg-HCO_3 type to Na-Cl type, typical for long-range flow paths in sedimentary basins.

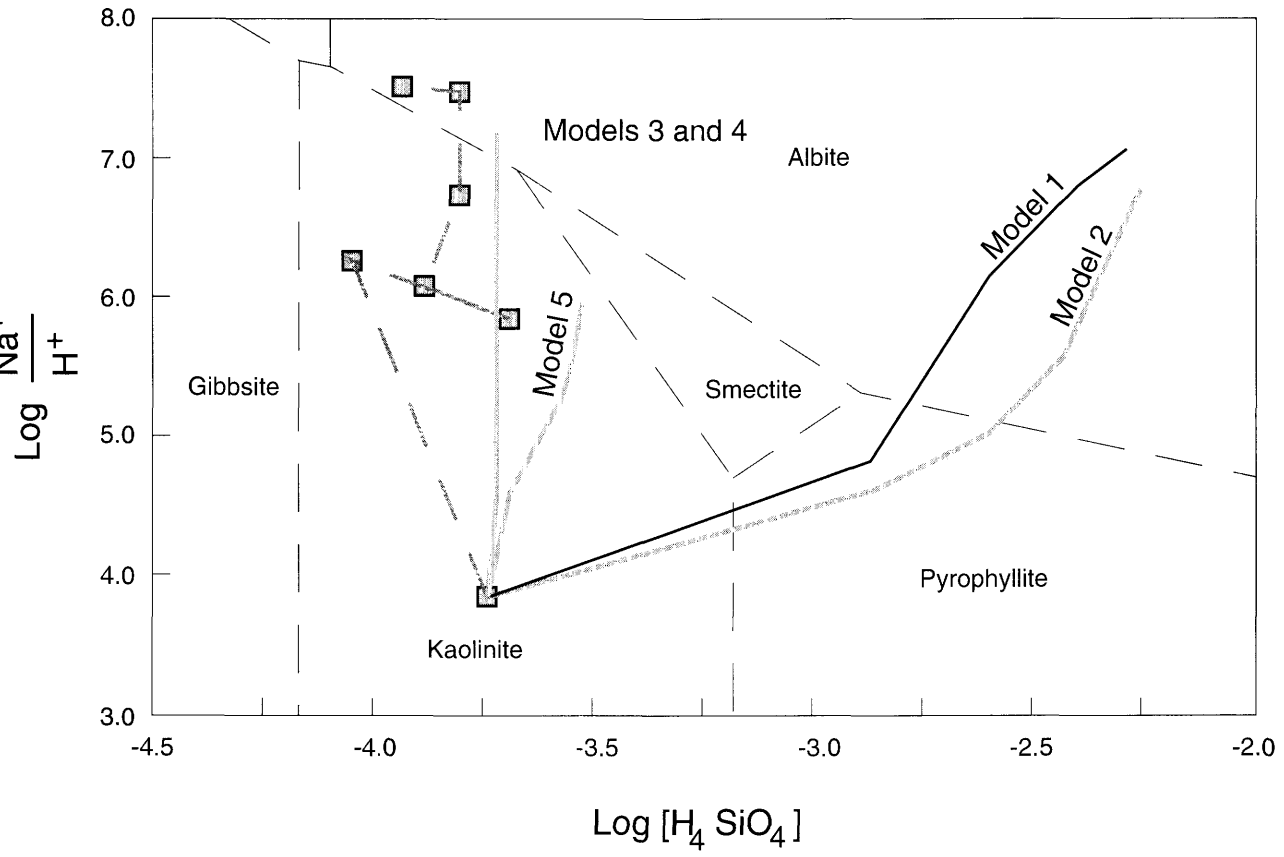

Figure 13. Results of models 1–5 for flow-path 3. Phase boundaries on the activity-activity diagram are from Drever (1982) and are constructed for 25 °C. Squares represent samples along flow-path 3 (see fig. 1).

Updip waters have near-neutral pH and low total dissolved solids contents (TDS) (less than 5,000 ppm), whereas downdip waters have higher pH, generally between 8 and 9, and much higher TDS contents (as much as 75,000 ppm). Computer modeling of ground-water chemical evolution used published analytical data and a modern thermodynamic data base. Preferred (though nonunique) solutions are consistent with petrographic and mineralogic observations. Thermodynamic calculations indicate that ground water in recharge zones is in equilibrium with observed authigenic kaolinite and is also capable of promoting the observed dissolution of feldspar. Feldspar dissolution probably supplies necessary soluble components for forming other diagenetic phases, including carbonate and clay minerals, observed in deeper rocks. Feldspar dissolution drives precipitation of carbonate minerals by contributing calcium to the solution and, more importantly, by increasing the pH of the water. Calcite precipitation buffers the pH and prevents it from rising above about 9. At all points along the flow path, silica concentrations most likely are controlled by the solubility of chalcedony, even though quartz is the thermodynamically stable phase.

Future studies should be directed at determining the source of the extreme salinity of the deep-basin waters. Trace-element and isotopic data may help to shorten the list of possible salt sources. The chemical models described herein are a useful starting point, but future studies should attempt to construct mass-balanced models integrating additional data for the hydrologic regime with observed changes in water chemistry.

REFERENCES CITED

Bodine, M.W., Jr., and Jones, B.F., 1986, The Salt Norm—A quantitative chemical-mineralogical characterization of natural waters: U.S. Geological Survey Water Resources Investigations Report 86–4086, 130 p.

Cole, R.D., and Picard, M.D., 1981, Sulfur isotope variations in marginal-lacustrine rocks of the Green River Formation, Colorado and Utah: Society of Economic Paleontologists and Mineralogists Special Publication, v. 31, p. 261–275.

Conroy, L.S., and Fields, F.K., 1977, Climatologic and hydrologic data, southeastern Uinta basin, Utah and Colorado, water years 1975 and 1976: Utah Department of Natural Resources Basic-Data Release 29, 244 p.

Drever, J.I., 1982, The geochemistry of natural waters: Englewood Cliffs, N.J., Prentice-Hall, 388 p.

Fouch, T.D., 1975, Lithofacies and related hydrocarbon accumulations in Tertiary strata of the western and central Uinta basin, Utah, *in* Bolyard, D.W., ed., Symposium on

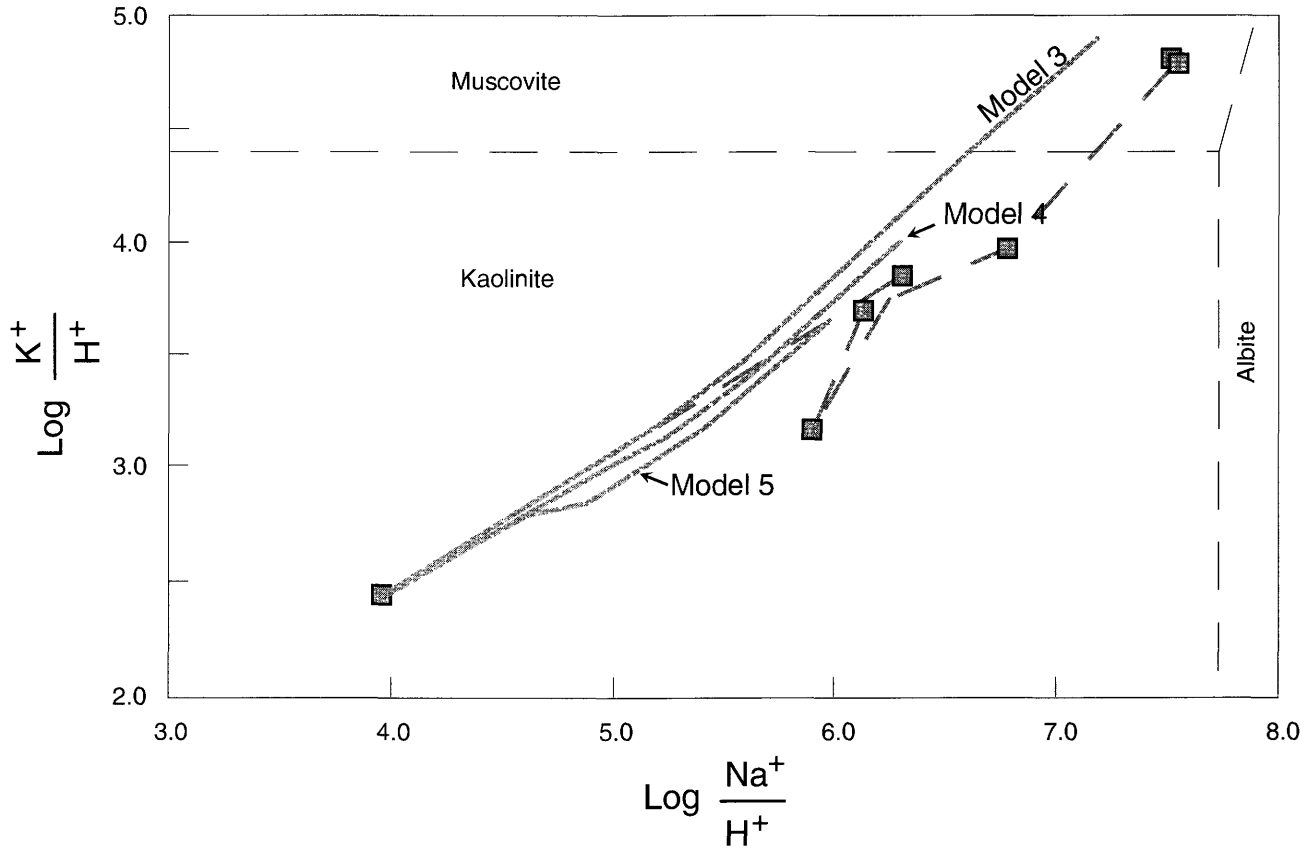

Figure 14. Results of models 3–5 for flow-path 3. Phase boundaries on the activity-activity diagram are from Drever (1982) and are constructed for 25 °C. Squares represent samples along flow-path 3 (see fig. 1).

Deep Drilling Frontiers in the Central Rocky Mountains: Rocky Mountain Association of Geologists, p. 163–173.

Franczyk, K.J., Pitman, J.K., Cashion, W.B., Dyni, J.R., Fouch, T.D., Johnson, R.C., Chan, M.A., Donnell, J.R., Lawton, T.F., and Remy, R.R., 1989, Evolution of resource-rich foreland and intermontane basins in eastern Utah and western Colorado: International Geological Congress, 28th, Guidebook T324, American Geophysical Union, 53 p.

Hanor, J.S., and McManus, K.M., 1988, Sediment alteration and clay mineral diagenesis in a regional ground water flow system, Mississippi Gulf Coastal Plain: Transactions, Gulf Coast Association of Geological Societies, v. 38, p. 495–502.

Harrison, A.G., and Thode, H.G., 1958, Sulphur isotope abundances in hydrocarbons and source rocks of the Uinta basin, Utah: American Association of Petroleum Geologists Bulletin, v. 42, p. 2642–2649.

Hood, J.W., Mundorff, J.C., and Price, D., 1976, Selected hydrologic data, Uinta basin area, Utah and Colorado: Utah Department of Natural Resources Basic-Data Release 26, 321 pp.

Kharaka, Y.K., Gunter, W.D., Aggarwal, P.K., Perkins, E.H., and DeBraal, J.D., 1988, SOLMINEQ.88–A computer program for geochemical modeling of water-rock interactions: U.S. Geological Survey Water-Resources Investigations 88–4227, 420 p.

Lee, R.W., 1985, Geochemistry of groundwater in Cretaceous sediments of the southeastern coastal plain of eastern Mississippi and western Alabama: Water Resources Research, v. 21, p. 1545–1556.

Mauger, R.L., 1972, A sulfur isotope study of bituminous sands from the Uinta basin, Utah: International Geology Congress, 24th, Proceedings, Comptes Rendus, sec. 5, p. 19–27.

Merino, E., 1975a, Diagenesis in Tertiary sandstones from Kettleman North Dome, California, I, Diagenetic mineralogy: Journal of Sedimentary Petrology, v. 45, p. 320–336.

_____ 1975b, Diagenesis in Tertiary sandstones from Kettleman North Dome, California, II, Interstitial solutions—Distribution of aqueous species at 100 °C and chemical relation to diagenetic mineralogy: Geochimica et Cosmochimica Acta, v. 39, p. 1629–1645.

Parkhurst, D.L., Plummer, L.N., and Thorstenson, D.C., 1980, PHREEQE—A computer program for geochemical calculations: U.S. Geological Survey Water-Resources Investigations 80–96, 210 p.

_____ 1982, BALANCE—A computer program for calculating mass transfer for geochemical reactions in ground water: U.S. Geological Survey Water-Resources Investigations 82–14, 29 p.

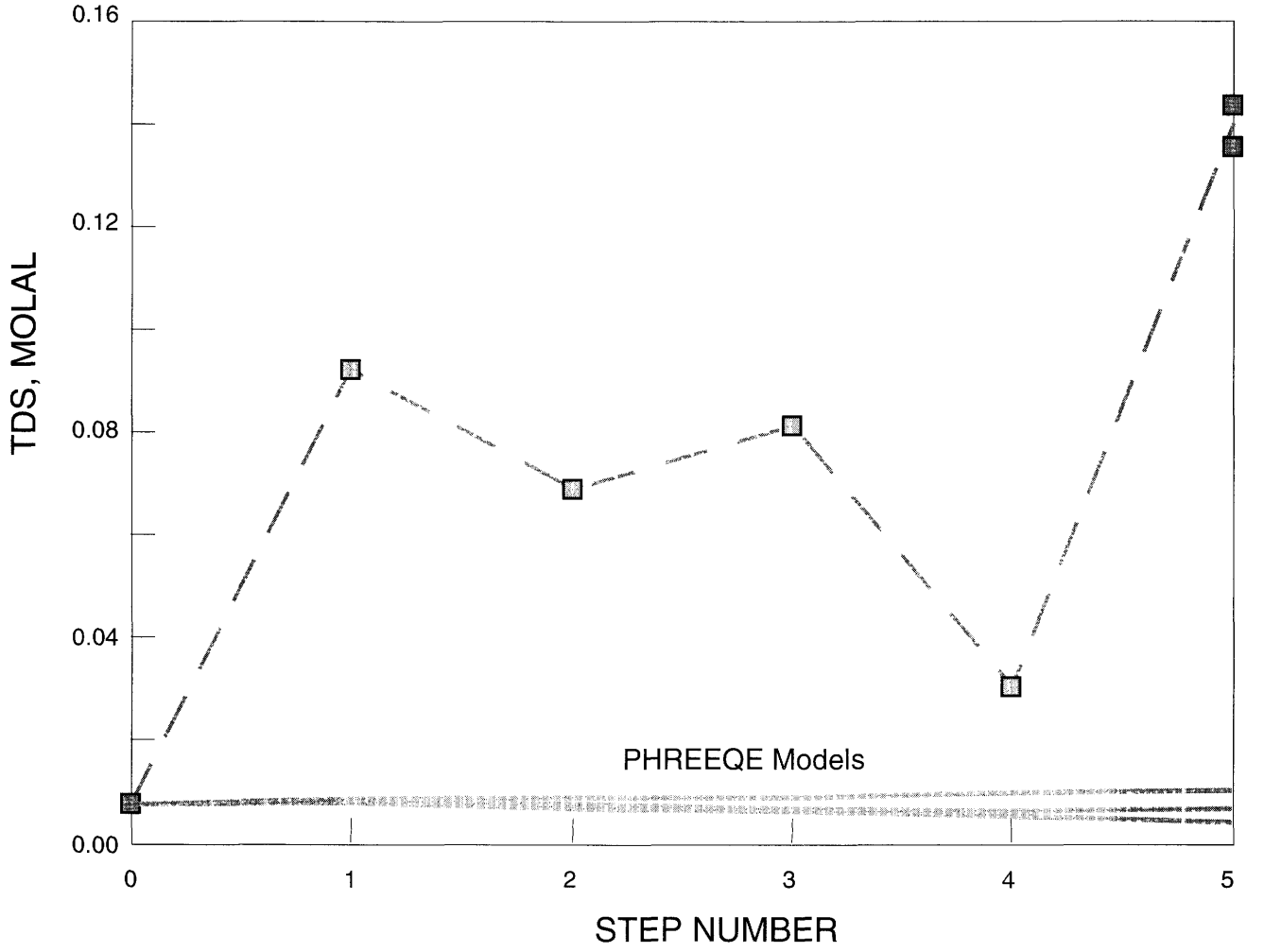

Figure 15. Total dissolved solids (TDS) along flow-path 3, as compared to the predictions using PHREEQE (solid lines). TDS is given in total molality of solutes. Squares represent samples along flow-path 3 (see fig. 1).

Pitman, J.K., Anders, D.E., Fouch, T.D., and Nichols, D.J., 1986, Hydrocarbon potential of nonmarine Upper Cretaceous and Lower Tertiary rocks, eastern Uinta basin, Utah, *in* Spencer, C.W., and Mast, R.F., eds., Geology of tight gas reservoirs: American Association of Petroleum Geologists Studies in Geology 24, p. 235–252.

Pitman, J.K., Fouch, T.D., and Goldhaber, M.B., 1982, Depositional setting and diagenetic evolution of some Tertiary unconventional reservoir rocks, Uinta basin, Utah: American Association of Petroleum Geologists Bulletin, v. 66, p. 1581–1596.

Price, D., and Miller, L.L., 1975, Hydrologic reconnaissance of the southern Uinta basin, Utah and Colorado: Utah Department of Natural Resources Technical Publication 49, 66 p.

Ryder, R.T., Fouch, T.D., and Elison, J.H., 1976, Early Tertiary sedimentation in the western Uinta basin: Geological Society of America Bulletin v. 87, p. 496–512.

Tuttle, M.L., 1988, Geochemical evolution and depositional history of sediment in modern and ancient saline lakes—Evidence from sulfur geochemistry: Golden, Colorado School of Mines, Ph. D. thesis, 312 p.

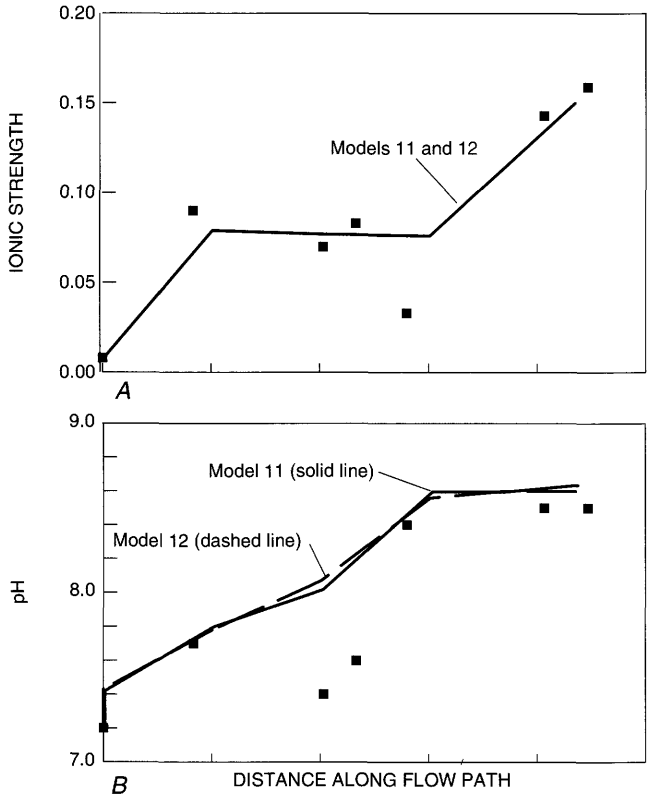

Figure 16. Predicted variations in pH (*A*) and ionic strength (*B*) according to models 11 and 12. Data points shown are for samples along flow-path 3.

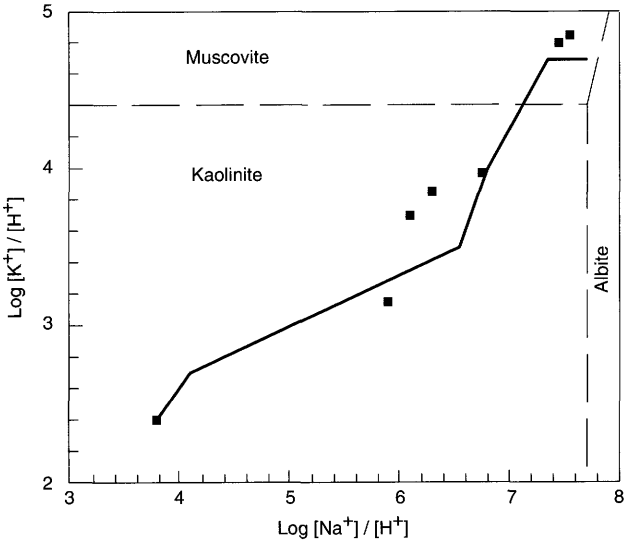

Figure 17. Chemical evolution of ground water in Na^+/H^+ versus K^+/H^+ space, as predicted by models 11 and 12. Data points shown are for samples along flow-path 3.

Appendix—List of unique field-identification numbers and sample dates for water analyses meeting criteria for completeness and accuracy described in the text

Using this list of ID numbers, the reader can consult the appropriate source reference to obtain the complete analysis. The sample numbers in the format GR-XX are the sample numbers designated in this study. Local ID refers to the sample number given in the source reference, which, along with the sample date or depth, uniquely identifies the sample. Dates are in the format YY-MM-DD; depths are in meters.

Sample No.	Local ID	Sample date	Sample No.	Local ID	Sample date
		Samples from Hood and others (1976)			
GR-01	(D-6-21)27cdc-1	65-03-08	GR-101	(D-9-20)36ddc-1	69-7-29
GR-02	(D-6-21)33adc-1	65-04-20	GR-102	(D-9-20)36ddc-1	69-7-30
GR-03	(D-6-21)33adc-1	65-04-20	GR-103	(D-9-20)36ddc-1	69-7-31
GR-04	(D-6-21)34bdc-1	65-01-16	GR-104	(D-9-20)36ddc-1	69-7-31
GR-05	(D-6-21)34bdc-1	65-01-16	GR-105	(D-10-16)11acd-1	64-10-1
GR-06	(D-6-21)35bbb-1	65-03-04	GR-106	(D-10-16)11acd-1	64-10-18
GR-07	(D-7-22)14bba-1	70-05-01	GR-107	(D-10-16)11dac-1	63-04-00
GR-08	(D-7-22)22aac-1	70-05-01	GR-108	(D-10-19)1cbd-1	63-10-15
GR-09	(D-7-22)22acc-1S	70-05-01	GR-109	(D-10-20)4ccb-1	63-07-00
GR-10	(D-7-22)22bab-1	70-05-01	GR-110	(D-11-15)2ccc-1	67-10-3
GR-11	(D-7-22)22cca-1	71-06-15	GR-111	(D-14-20)30bab-1	63-7-22
GR-12	(D-7-22)25cad-1	65-07-07	GR-112	U(C-1-1)8acd-1	63-11-7
GR-13	(D-7-22)28cca-1	70-03-27	GR-113	U(C-1-1)8acd-1	63-11-30
GR-14	(D-7-22)29abb-1	71-07-16	GR-114	U(C-1-1)13ccd-1	60-05-04
GR-15	(D-7-22)29cab-1	70-05-29	GR-115	U(C-1-2)3bcd-1	67-12-04
GR-16	(D-7-22)29cab-1	70-05-29	GR-116	U(C-1-2)7cac-1	70-01-23
GR-17	(D-7-22)29cac-1	68-11-01	GR-117	U(C-1-2)7cac-1	70-01-24
GR-18	(D-7-22)34bac-1	65-06-16	GR-118	U(C-1-2)7cac-1	70-01-25
GR-19	(D-7-23)13bab-1	69-01-31	GR-119	U(C-1-2)7cac-1	70-01-26
GR-20	(D-7-23)14cdd-1	65-01-15	GR-120	U(C-1-2)7cac-1	70-01-27
GR-21	(D-7-23)14dad-1	69-01-31	GR-121	U(C-1-2)7cac-1	70-05-06
GR-22	(D-7-23)25aab-1	70-12-30	GR-122	U(C-1-2)11bba-1	67-10-02
GR-23	(D-7-23)27ccc-1	69-02-03	GR-123	U(C-1-2)11bba-1	67-10-03
GR-24	(D-7-23)28cad-1	69-02-03	GR-124	U(C-1-2)11bba-1	67-12-04
GR-25	(D-7-23)29ccc-1	69-09-18	GR-125	U(C-1-2)11bba-1	68-4-26
GR-26	(D-7-23)29ccc-1	69-09-18	GR-126	U(C-1-2)7cac-1s	69-4-18
GR-27	(D-7-24)28acd-1	66-01-06	GR-127	U(C-1-2)7cac-1s	70-2-26
GR-28	(D-7-24)31acb-1	63-04-17	GR-128	U(C-3-6)8bba-1	68-9-16
GR-29	(D-7-24)36aaa-1	65-03-02	GR-129	U(C-3-6)18bbd-1	65-9-30
GR-30	(D-8-21)29bcc-1	69-07-16	GR-130	U(C-3-6)18bbd-1	65-10-1
GR-31	(D-8-21)29bcc-1	65-02-12	GR-131	U(C-3-6)18bbd-1	65-11-1
GR-32	(D-8-21)29bcc-1	65-05-27	GR-132	U(C-3-6)18bbd-1	65-11-19
GR-33	(D-8-22) 4dcd-1	65-04-08	GR-133	U(C-3-6)18bbd-1	66-1-7
GR-34	(D-8-23)18dbb-1	65-03-04	GR-134	U(C-3-6)20acb-1	69-10-22
GR-35	(D-10-22)17aad1S	64-05-11	GR-135	U(C-3-7)22acd-1	70-3-26
GR-36	(D-11-21)31bdd-1	71-08-31	GR-136	U(C-3-7)22acd-1	70-3-27
GR-37	(D-11-24) 8caa-1	61-09-06	GR-137	U(C-3-7)22acd-1	70-4-9
GR-38	(D-13-23)26acd-1	60-06-00	GR-138	U(C-4-1)13dad-1	69-4-10
GR-39	U(D-1-1)21cbd-1	67-08-24	GR-139	U(C-4-1)13dad-1	69-4-10
GR-40	U(D-1-1)21dbc-1	59-11-05	GR-140	U(C-4-5)10bdd-1s	72-1-4
			GR-141	U(C-4-9)16dba-1	71-1-25
			GR-142	U(C-4-11)33bda-s1	71-10-21

Appendix—List of unique field-identification numbers and sample dates for water analyses meeting criteria for completeness and accuracy described in the text—Continued

Sample No.	Local ID	Sample date	Sample No.	Local ID	Sample date
		Samples from Conroy and Fields (1977)			
GR-143	(D-10-20)35bbc-1	74-8-20	GR-187	(D-10-24)20aad-2	75-3-13
GR-144	(D-10-21)2aca-1	75-6-25	GR-188	(D-10-24)20aad-2	75-9-11
GR-145	(D-10-21)16add-1	74-8-21	GR-189	(D-10-24)20aad-2	75-9-12
GR-146	(D-10-21)16add-1	75-6-25	GR-190	(D-10-24)20aad-2	75-11-13
GR-147	(D-10-22)17aad-1	74-8-21	GR-191	(D-10-24)20aad-2	76-6-26
GR-148	(D-10-22)17aad-1	75-6-25	GR-192	(D-10-24)25caa-1	74-11-21
GR-149	(D-10-24)12bdb-1	75-11-12	GR-193	(D-10-24)25caa-1	74-12-10
GR-150	(D-10-24)12bdb-1	76-6-24	GR-194	(D-10-24)25caa-1	75-3-12
GR-151	(D-10-24)12bdb-1	76-9-14	GR-195	(D-10-24)25caa-1	75-11-11
GR-152	(D-10-24)12cda-1	74-11-20	GR-196	(D-10-24)28ddb-1	75-12-10
GR-153	(D-10-24)12cda-1	75-3-18	GR-197	(D-10-24)36dcd-1	74-11-19
GR-154	(D-10-24)12cda-1	75-5-13	GR-198	(D-10-24)36dcd-1	75-11-10
GR-155	(D-10-24)12cda-1	75-6-26	GR-199	(D-10-25)19dda-1	75-11-12
GR-156	(D-10-24)12cda-1	75-8-30	GR-200	(D-10-25)19dda-1	76-9-14
GR-157	(D-10-24)12cda-1	75-11-14	GR-201	(D-11-21)31bdd-1	74-8-20
GR-158	(D-10-24)12cda-1	76-6-24	GR-202	(D-11-23)13dcd-1	75-6-26
GR-159	(D-10-24)13adb-1	75-11-12	GR-203	(D-11-24)6dbc-1	74-9-10
GR-160	(D-10-24)13adb-1	76-6-24	GR-204	(D-11-24)6dbc-1	75-6-26
GR-161	(D-10-24)13adb-1	76-9-16	GR-205	(D-11-24)7cac-1	74-9-10
GR-162	(D-10-24)13adb-2	74-11-19	GR-206	(D-11-24)7cac-1	75-6-26
GR-163	(D-10-24)13adb-2	74-11-21	GR-207	(D-11-24)8caa-1	74-9-10
GR-164	(D-10-24)13adb-2	75-3-13	GR-208	(D-11-25)7dac-1	75-3-12
GR-165	(D-10-24)13adb-2	75-11-12	GR-209	(D-11-25)7dac-1	75-11-11
GR-166	(D-10-24)13adb-2	76-6-24	GR-210	(D-11-25)21cca-1	75-3-12
GR-167	(D-10-24)13adb-2	76-9-16	GR-211	(D-11-25)21cca-1	75-11-11
GR-168	(D-10-24)13ccc-1	74-11-22	GR-212	(D-13-25)13add-s1	74-9-12
GR-169	(D-10-24)13ccc-1	74-12-13	GR-213	(D-14-22)25cac-s1	74-8-21
GR-170	(D-10-24)13ccc-1	75-3-14	GR-214	(D-14-24)21ccc-s1	74-8-23
GR-171	(D-10-24)13ccc-1	75-11-13	GR-215	(D-15-20)15bbd-s1	75-6-17
GR-172	(D-10-24)13ccc-1	76-3-21	GR-216	(D-15-23)36ddd-s1	75-6-18
GR-173	(D-10-24)13ccc-1	76-6-30	GR-217	(D-15-25)7bcc-s1	74-8-22
GR-174	(D-10-24)13ccc-1	76-9-14	GR-218	(D-15-25)13bad-s1	74-9-11
GR-175	(D-10-24)20aad-1	75-3-13	GR-219	(D-15-25)18cda-s1	76-9-16
GR-176	(D-10-24)20aad-1	75-5-12	GR-220	(D-16-19)18cbc-s1	74-8-20
GR-177	(D-10-24)20aad-1	75-6-24	GR-221	(D-16-22)23dad-s1	74-8-22
GR-178	(D-10-24)20aad-1	75-7-27	GR-222	(D-16-23)16bbd-s1	74-8-22
GR-179	(D-10-24)20aad-1	75-8-18	GR-223	(D-17-19)9acb-s1	75-6-17
GR-180	(D-10-24)20aad-1	75-8-19	GR-224	(D-17-19)28bab-s1	74-8-20
GR-181	(D-10-24)20aad-1	75-11-13	GR-225	(D-17-21)10bdd-s1	75-6-19
GR-182	(D-10-24)20aad-1	76-3-17	GR-226	(D-17-22)19bbd-s1	74-8-22
GR-183	(D-10-24)20aad-1	76-6-26	GR-227	(D-18-20)7bad-s1	74-8-20
GR-184	(D-10-24)20aad-1	76-9-19	GR-228	(D-19-19)36caa-s1	75-6-17
GR-185	(D-10-24)20aad-2	74-11-27	GR-229	S(C-5-104)36cad-s1	74-9-11
GR-186	(D-10-24)20aad-2	74-12-11			

Appendix—List of unique field-identification numbers and sample dates for water analyses meeting criteria for completeness and accuracy described in the text—Continued

Sample No.	Local ID	Sample depth	Sample No.	Local ID	Sample depth
		Samples from Price and Miller (1975)			
GR-41	(D-9-20)36ddc-1	690-1,028	GR-57	(D-10-20)7cdb-1	1,131-1,145
GR-42	(D-9-20)36ddc-1	690-1,079	GR-58	(D-10-20)8cab-1	1,207-1,216
GR-43	(D-9-20)36ddc-1	690-1,179	GR-59	(D-10-20)8cab-1	1,272-1,281
GR-44	(D-9-20)36ddc-1	690-1,179	GR-60	(D-10-21)16add-1	690-1,283
GR-45	(D-10-16)11acd-1	1,563-1,575	GR-61	(D-10-23)24bba-1	1,118
GR-46	(D-10-16)16acd-1	1,318-1,329	GR-62	(D-11-21)14baa-1	231-237
GR-47	(D-10-17)30bbd-1	1,377-1,381	GR-63	(D-11-16) 3bbc-1	1,502-1,520
GR-48	(D-10-17)30bbd-1	1,484-1,500	GR-64	(D-11-16) 3bbc-1	1,530-1,538
GR-49	(D-10-18)13cdb-1	1,475-1,487	GR-65	(D-11-24) 8caa-1	465
GR-50	(D-10-18)14-bbd-1	788-832	GR-66	(D-14-20)30bab-1	686-696
GR-51	(D-10-18)14-bbd-1	1,342-1,366	GR-67	U(C-4-1)13dad-1	1,465-1,487
GR-52	(D-10-18)14-bbd-1	1,413-1,427	GR-68	U(C-4-1)13dad-1	1,874-1,934
GR-53	(D-10-18)14-bbd-1	1,542-1,571	GR-69	U(C-4-4)13dda-1	2,140-2,164
GR-54	(D-10-19)1cbd-1	1,039-1,048	GR-70	U(C-4-4)16aca-1	1,010-1,221
GR-55	(D-10-20)4ccb-1	1,057-1,094	GR-71	U(C-4-5)10bdd-1	2,309-2,363
GR-56	(D-10-20)7cdb-1	755-764	GR-72	U(C-6-6)35bdd-1	1,163-1,188

☆U.S. GOVERNMENT PRINTING OFFICE: 1991- 573-049/46010

SELECTED SERIES OF U.S. GEOLOGICAL SURVEY PUBLICATIONS

Periodicals

Earthquakes & Volcanoes (issued bimonthly).
Preliminary Determination of Epicenters (issued monthly).

Technical Books and Reports

Professional Papers are mainly comprehensive scientific reports of wide and lasting interest and importance to professional scientists and engineers. Included are reports on the results of resource studies and of topographic, hydrologic, and geologic investigations. They also include collections of related papers addressing different aspects of a single scientific topic.

Bulletins contain significant data and interpretations that are of lasting scientific interest but are generally more limited in scope or geographic coverage than Professional Papers. They include the results of resource studies and of geologic and topographic investigations; as well as collections of short papers related to a specific topic.

Water-Supply Papers are comprehensive reports that present significant interpretive results of hydrologic investigations of wide interest to professional geologists, hydrologists, and engineers. The series covers investigations in all phases of hydrology, including hydrogeology, availability of water, quality of water, and use of water.

Circulars present administrative information or important scientific information of wide popular interest in a format designed for distribution at no cost to the public. Information is usually of short-term interest.

Water-Resources Investigations Reports are papers of an interpretive nature made available to the public outside the formal USGS publications series. Copies are reproduced on request unlike formal USGS publications, and they are also available for public inspection at depositories indicated in USGS catalogs.

Open-File Reports include unpublished manuscript reports, maps, and other material that are made available for public consultation at depositories. They are a nonpermanent form of publication that may be cited in other publications as sources of information.

Maps

Geologic Quadrangle Maps are multicolor geologic maps on topographic bases in 7 1/2- or 15-minute quadrangle formats (scales mainly 1:24,000 or 1:62,500) showing bedrock, surficial, or engineering geology. Maps generally include brief texts; some maps include structure and columnar sections only.

Geophysical Investigations Maps are on topographic or planimetric bases at various scales; they show results of surveys using geophysical techniques, such as gravity, magnetic, seismic, or radioactivity, which reflect subsurface structures that are of economic or geologic significance. Many maps include correlations with the geology.

Miscellaneous Investigations Series Maps are on planimetric or topographic bases of regular and irregular areas at various scales; they present a wide variety of format and subject matter. The series also includes 7 1/2-minute quadrangle photogeologic maps on planimetric bases which show geology as interpreted from aerial photographs. Series also includes maps of Mars and the Moon.

Coal Investigations Maps are geologic maps on topographic or planimetric bases at various scales showing bedrock or surficial geology, stratigraphy, and structural relations in certain coal-resource areas.

Oil and Gas Investigations Charts show stratigraphic information for certain oil and gas fields and other areas having petroleum potential.

Miscellaneous Field Studies Maps are multicolor or black-and-white maps on topographic or planimetric bases on quadrangle or irregular areas at various scales. Pre-1971 maps show bedrock geology in relation to specific mining or mineral-deposit problems; post-1971 maps are primarily black-and-white maps on various subjects such as environmental studies or wilderness mineral investigations.

Hydrologic Investigations Atlases are multicolored or black-and-white maps on topographic or planimetric bases presenting a wide range of geohydrologic data of both regular and irregular areas; principal scale is 1:24,000 and regional studies are at 1:250,000 scale or smaller.

Catalogs

Permanent catalogs, as well as some others, giving comprehensive listings of U.S. Geological Survey publications are available under the conditions indicated below from the U.S. Geological Survey, Books and Open-File Reports Section, Federal Center, Box 25425, Denver, CO 80225. (See latest Price and Availability List.)

"Publications of the Geological Survey, 1879-1961" may be purchased by mail and over the counter in paperback book form and as a set of microfiche.

"Publications of the Geological Survey, 1962-1970" may be purchased by mail and over the counter in paperback book form and as a set of microfiche.

"Publications of the U.S. Geological Survey, 1971-1981" may be purchased by mail and over the counter in paperback book form (two volumes, publications listing and index) and as a set of microfiche.

Supplements for 1982, 1983, 1984, 1985, 1986, and for subsequent years since the last permanent catalog may be purchased by mail and over the counter in paperback book form.

State catalogs, "List of U.S. Geological Survey Geologic and Water-Supply Reports and Maps For (State)," may be purchased by mail and over the counter in paperback booklet form only

"Price and Availability List of U.S. Geological Survey Publications," issued annually, is available free of charge in paperback booklet form only.

Selected copies of a monthly catalog "New Publications of the U.S. Geological Survey" available free of charge by mail or may be obtained over the counter in paperback booklet form only. Those wishing a free subscription to the monthly catalog "New Publications of the U.S. Geological Survey" should write to the U.S. Geological Survey, 582 National Center, Reston, VA 22092.

Note.--Prices of Government publications listed in older catalogs, announcements, and publications may be incorrect. Therefore, the prices charged may differ from the prices in catalogs, announcements, and publications.


U.S. DEPARTMENT OF THE INTERIOR
March 3, 1849